Subtype-specific circadian clock dysregulation modulates breast cancer biology, invasiveness, and prognosis

Jan A Hammarlund[1,#], Shi-Yang Li[2, #], Gang Wu[3, #], Jia-wen Lian[1], Sacha J Howell[4], Rob Clarke[4], Antony Adamson[1], Cátia F. Gonçalves[1], John B Hogenesch[3], Qing-Jun Meng[2, *], Ron C Anafi[5, *]

[1]School of Biomedical Engineering, Science and Health Systems. Drexel University, Philadelphia, PA, USA
[2]Division of Cell Matrix Biology and Regenerative Medicine, School of Biological Sciences, Faculty of Biology, Medicine and Health, University of Manchester, Manchester, UK
[3]Divisions of Human Genetics and Immunobiology, Center for Circadian Medicine, Department of Pediatrics, Cincinnati Children's Hospital Medical Center, Cincinnati, OH, USA.
[4]Breast Biology Group, Manchester Breast Centre, Division of Cancer Sciences, Faculty of Biology, Medicine and Health, University of Manchester, Manchester, UK.
[5]Department of Medicine, Chronobiology and Sleep Institute, Perelman School of Medicine, University of Pennsylvania, Philadelphia, PA USA.

[#], These authors contributed equally.
*, Joint senior corresponding authors: Ron C. Anafi (ron.anafi@pennmedicine.upenn.edu) and Qing-Jun Meng (qing-jun.meng@manchester.ac.uk).

Summary

Studies in shift workers and model organisms link circadian disruption to breast cancer. However, molecular rhythms in non-cancerous and cancerous human breast tissues are largely unknown. We reconstructed rhythms informatically, integrating locally collected, time-stamped biopsies with public datasets. For non-cancerous tissue, the inferred order of core-circadian genes matches established physiology. Inflammatory, epithelial-mesenchymal transition (EMT), and estrogen responsiveness pathways show circadian modulation. Among tumors, clock correlation analysis demonstrates subtype-specific changes in circadian organization. Luminal A organoids and informatic ordering of Luminal A samples exhibit continued, albeit disrupted rhythms. However, CYCLOPS magnitude, a measure of global rhythm strength, varied widely among Luminal A samples. Cycling of EMT pathway genes was markedly increased in high-magnitude Luminal A tumors. Patients with high-magnitude tumors had reduced 5-year survival. Correspondingly, 3D Luminal A cultures show reduced invasion following molecular clock disruption. This study links subtype-specific circadian disruption in breast cancer to EMT, metastatic potential, and prognosis.

Keywords

Breast Cancer, Informatics, Circadian Data Ordering, Metastasis, Estrogen Receptor, Rhythm Strength, Prognosis, Circadian Medicine

Highlights

- Breast cancers exhibit subtype-specific and estrogen-dependent clock disorganization.
- Luminal A tumors show dysregulated rhythmic pathways and varied rhythm strength.
- Higher rhythm strength in Luminal A tumors was correlated with reduced 5-year survival.
- Reducing rhythm strength in Luminal A cells *in vitro* slows cell invasion.

Introduction

Worldwide, breast cancer is the most common cancer among women[1-3]. Over the last decades, the introduction of early detection programs, combined with improvements in systemic therapies, have reduced breast cancer mortality[2-4]. Despite these improvements, resistance and subsequent relapse remain major issues[3]. Among women, those with breast cancer lose more disability-adjusted life years than with any other cancer[5]. Adverse effects frequently compromise quality of life[3,6-8]. There remains a clear need to improve the therapeutic index for breast cancer treatments.

Over the last two decades, research has highlighted the critical roles of cell-intrinsic circadian rhythms in disease (including cancer) and medicine[9-12]. The circadian (~24-hourly) clock is evolutionarily ancient and highly conserved, permitting cells to anticipate daily environmental changes through temporally coordinated metabolic and gene expression profiles[13-15]. A series of transcription-translational feedback loops form the molecular circadian clock[13-16]. The positive arm of the central loop includes the transcriptional activators Circadian Locomotor Output Cycles Kaput (CLOCK) and Brain and Muscle ARNT-Like 1 (BMAL1)[13-16]. The negative arm, which includes the Cryptochrome (*Cry1/Cry2*) and Period (*Per1/Per2*) genes, later represses translation[13-16].

The influence of circadian time on cell division, and, by extension, cancer, is particularly strong. In yeast and mammals, evolutionary pressures acted to gate DNA replication and cell division, shielding the dividing cell from solar radiation and toxic metabolites[12,17,18]. The cell cycle and circadian clocks share components and signaling molecules and show reciprocal regulation[19-24]. In addition, several oncogenes have been causally linked to circadian clock dysfunctions and may directly hijack clock mechanisms[22,25].

Epidemiological and animal studies have proposed that night shift work that disrupts circadian rhythms may increase the risk of developing breast and other cancers[26-28]. This has prompted the WHO to classify night shift work as a probable carcinogen[26-28]. Previously we demonstrated that the extracellular microenvironment modulates functional, cell-intrinsic circadian clocks in mouse mammary gland tissue and human breast epithelial cells[29-32]. Time series transcriptomic analysis revealed hundreds of rhythmic genes in the mouse mammary gland. Rhythmic transcripts included critical molecules implicated in cell cycle regulation, epithelial/progenitor cell function, and hormone responsiveness. Acting, in part, through an immunosuppressive shift in the tumor environment, chronic circadian disruption increases mammary cancer cell dissemination and metastasis in a mouse model of tumorigenesis[33].

Beyond this basic biology, the molecular circadian clock regulates thousands of genes in a cell and tissue-specific manner. Half of the 100-best-selling-drugs target molecules that oscillate in different mouse tissues[16]. In 1973, Halberg and colleagues initiated a series of studies with the underlying hypothesis that dosage time could influence chemotherapeutic pharmacokinetics, limit toxicity, and improve efficacy[34]. Decades of clinical experience show that time-of-day can influence chemotherapeutic activity[35]. However, the widespread translation of circadian biology in oncology remains slow and serendipitous. Mechanistic knowledge about the unique molecular rhythms in distinct tumors and normal human tissues must be improved. Repeated biopsies or time course sampling from large numbers of human patients is neither safe nor practical. As a result, clinically relevant molecular rhythms still need to be discovered, and opportunities for targeted circadian therapies are unrealized. In addition, while some in vitro and in vivo cancer models demonstrate a complete lack of rhythms, other models (like U2OS cells) show continued rhythms[19]. Indeed, informatic analysis of intact hepatocellular carcinoma has shown disrupted yet persistent transcriptional rhythms[36].

We recently optimized CYClic Ordering by Periodic Structure (CYCLOPS) to overcome this problem. This machine learning algorithm has allowed us to reconstruct circadian rhythms in samples where sampling time is unknown[36-38]. We adapted CYCLOPS to better account for the non-circadian variation inherent to large-scale data in clinical databases (CYCLOPS 2.0). We then adopted a hybrid study design (Fig 1A). We combined deep sequencing of a small number of time-stamped, paired clinical samples with data from large RNASeq datasets—the Tissue Cancer Genome Atlas[39] (TCGA) and the Genotype-Tissue Expression[40] (GTEx) project—where the circadian time of sample collection is unknown. Both the modified CYCLOPS algorithm and experimental validation reveal clear cancer-subtype-dependent changes in molecular clocks and their rhythmic targets. Notably, we uncover a key role of molecular timekeeping in Luminal A tumors linking circadian rhythms to epithelial-mesenchymal transition (EMT), cell invasion, and prognosis. Our studies also provide mechanistic insights into the role of estrogen receptors (ER) in regulating breast cancer clocks.

Results

Profound changes in clock gene expression and circadian organization in time-recorded breast cancer biopsies

To assess and improve the accuracy of informatic predictions and to enable direct comparisons of transcriptional changes in circadian genes, we collected 43 pairs of fresh human breast samples (non-cancerous and paired tumors from the same individuals) from patients undergoing mastectomy at the Nightingale Breast Centre, Manchester, UK (Patient demographics on Table. 1). Non-cancerous tissues were collected at least 4 cm away from tumors (Fig. 1A). Tumor samples included Luminal A (N=29), Luminal B (N=3), HER2 (N=2) and Triple-negative breast cancers (TNBC, N=9) (Fig. 1B). Resection times of all samples were recorded (Fig. 1C). To identify non-cancerous and tumor areas we employed Hematoxylin and Eosin-Y staining (H&E staining) and immunohistochemistry using epithelial and stromal markers (Cytokeratin 8 and Vimentin, respectively) (Fig. 1D). Normal breast contains organized acinar and lobular structures, whereas tumor regions lack regular glandular structures. We performed RNA sequencing following RNA isolation. Based on these RNAseq data, the expression of most clock genes is significantly altered in breast cancer tissues. Compared to the paired non-cancerous samples, we observed significant downregulation of PER1, PER2, CRY2, HLF, TEF, and NFIL3 (Fig. 1E; Fig. S1). In contrast, CLOCK, NPAS2, CIART/CHRONO, BHLHE40, RORA, and RORC were significantly upregulated in these breast tumors (Fig. 1E; Fig. S1).

To examine core clock organization in these breast tumors, we performed Spearman's correlation coefficient analysis[38,41-43] using RNAseq data from time-stamped paired breast tumors and non-cancerous samples with a sequencing depth of >20 million reads. As expected, the non-cancerous breast tissues demonstrate core-clock correlation patterns mirroring those seen in mice[16]. The expression levels of clock activators positively correlate with each other across samples. The same is true for the canonical repressors. In contrast, the two groups negatively correlate with each other (Fig. 1F). The strong similarity between the clock correlation patterns seen in the non-cancerous tissue (Fig. 1F, Zstat score of 20.71) and the mouse model suggests a functional clock network. In contrast, a weaker overall correlation in breast tumors (Fig. 1F, Zstat score of 9.28) suggests a weakening of core circadian organization in these samples.

Transcriptional circadian rhythms are evolutionarily conserved in non-cancerous human breast and mouse mammary tissue

We adopted a hybrid study design[38] to evaluate circadian time order in human non-cancerous breast tissues. We used informatic tools to integrate RNAseq data from newly collected time-stamped breast samples (N=26, with non-cancerous samples with > 20 million reads) with RNAseq data from female breast samples in public databases. We incorporated data from TCGA[39] and GTEx[40] (Table S1). We did not

include samples collected in centers where only a small number (n<5) of non-cancerous samples were processed.

Systematic differences between sample collection sites, processing methods, and patient populations complicate the use of aggregate data. These differences may be particularly problematic when different centers have different biases in collection time. We modified the CYCLOPS[36] neural network to accommodate explicit confounding variables, simultaneously learning confounder adjustments and a common circular structure that explains the variance of the combined data: CYCLOPS 2.0 (Fig. S2A). We benchmarked CYCLOPS 2.0 on actual, semi-synthetic, and fully-synthetic data with different temporal biases (Fig. S2B-D). CYCLOPS 2.0 demonstrates improved accuracy with realistic levels of non-circadian noise. Finally, we allowed the ordering process to use information from a subset of time-stamped samples. We performed 10-fold cross-validation to determine the relative weight given to predicting time in these samples and identify a common circular structure for all samples.

We identified the human orthologues of transcripts that cycle in mouse mammary gland tissue[29]. Combining these with the human orthologues of transcripts that cycled in >75% of mouse tissues[16], we constructed a circadian "seed gene" list appropriate for ordering human breast tissue. Ordering the combined dataset using these seed genes and including temporal information from the 26 time-stamped human samples, the CYCLOPS smoothness and ordering metrics for the entire dataset meet previously established standards (Statsmooth=0.75, Staterror=0.015). The CYCLOPS-predicted sample phases show a significant correlation with the known sample collection times of the 26 subjects (Corrcirc=0.7, p<0.005) (Fig. 2A). As expected, the clinical biopsies available in TCGA show a temporal bias in inferred sample collection phase (Fig. 2B). In contrast, the distribution of inferred sample phases assigned to the GTEx samples (autopsy collection) was more uniform (Fig. 2B). After ordering, we used modified Cosinor regression[36,44] to identify cycling transcripts and estimate their amplitude and acrophase (time of peak expression) (Fig. 2C, D). The expanded Cosinor model explicitly accounted for differences in expression due to sequencing sites or source databases. At a BHq threshold of 0.05, we identified ~2,000 genes as rhythmic. When we imposed a relative cycling amplitude (amplitude/MESOR (Midline Estimating Statistic of Rhythm)) greater than 1/3—as a measure of likely biological significance—we reduced the number of identified cycling transcripts to ~650 (File. S2). As observed in other tissues, there are clear circadian "rush hour periods" where many rhythmic transcripts peaked[16,37,45]. With the notable exception of RORC, the relative acrophases of core-clock transcripts reconstructed from non-cancerous human breast tissue are in good accord with the well-established ordering of these transcripts in other mouse and human tissues (Fig. 2E).

To put these cycling results in a broader biological context, we used phase set enrichment (PSEA)[46] to identify annotated gene sets and biological pathways where the constituent cycling transcripts exhibited circadian concentration and were not uniformly distributed across the circadian day. Pathways related to

adipogenesis, EMT, and estrogen responsiveness, show circadian orchestration, similar to reports from mouse mammary gland (Fig. 2F). Using both gene set enrichment[47] and over-representation approaches[48-50], we also labeled pathways that were enriched for cycling genes. In addition to the abovementioned pathways, various immune and cell cycle pathways show marked circadian orchestration (Fig. 2G, H).

ER activity correlates with circadian organization and function in breast cancer subtypes

Our clock correlation analysis on locally collected cancer samples combined data from biologically distinct breast tumor types. We applied clock gene correlation analysis[38,41-43] to TCGA breast tumor data to evaluate cancer-subtype-dependent changes in clock organization—the expression of the PAM50 panel genes defined cancer subtypes[51,52]. Consistent with the non-cancerous time-stamped samples, the non-cancerous breast tissues from the database show an intact core circadian organization that closely mirrors the established consensus with a Zstat score of 20.86. The Luminal A samples demonstrate weaker but still considerable evidence of intact circadian organization with a Zstat score of 11.04. On the other hand, Luminal B and Triple Negative breast cancers exhibit disrupted correlation patterns with Zstat scores of 6.93 and 4.98, respectively (Fig. 3A). The relatively small number of HER2 samples in the TCGA database prevented evaluation of clock organization in this tumor type.

Given these findings, we hypothesized that circadian function in breast tumor tissues, like core clock organization, varies among cancer subtypes - with Luminal A samples showing reasonably good clocks. We assessed molecular circadian rhythms in breast tumors and paired non-cancerous tissues from the same individuals to confirm these predictions. We derived organoids from primary mammary epithelial cells. This model more closely mimics in vivo physiological functions of mammary epithelia[31,32,53]. The organoid cultures from normal breast tissues showed typical acinar structures. In contrast, breast tumor organoids showed disrupted cell polarity (Fig. 3B). After lentiviral transduction of a BMAL1-Luc circadian reporter, we imaged bioluminescence signals using an LV200 imaging system (Olympus). Non-cancerous human mammary organoids showed robust circadian rhythms. Patient-derived Luminal A tumor organoids showed persistent but weakened rhythms (Fig. 3C, Video. S1, N=4). However, we did not observe sustained circadian rhythms in BMAL1-Luc activity in TNBC tumor organoids (Fig. 3D, Video. S2, N=3), Luminal B organoids, or HER2 organoids (data not shown). Using either a BMAL1-Luc reporter or time course western blot studies of clock factors, we also observed corresponding clock changes in established breast cancer cell lines representing various tumor subtypes (Fig. S3A-C). The MCF-7 cell line (representative of ER+ Luminal A) continues to exhibit circadian rhythms, while the MDA-MB-231 (TNBC) and SKBR3 (HER2+) cell lines do not (Fig. S3B, C). In unsynchronized cells, we observed altered average expression levels of core clock genes among the three cell lines. (Fig. S3D).

As ER status is one of the key factors in differentiating these tumor subtypes, our informatic and experimental results suggest a possible link between ER responsiveness and clock functions in breast

cancer cells. Indeed, further stratification of breast tumor samples based on ER status indicates a strong correlation between ER expression and clock functionality (Fig. S4A). To more directly determine whether ER signaling regulates circadian rhythms in breast cancer cells, ERα was knocked out of BMAL1-Luc MCF-7 cells using CRISPR-Cas9. Following co-transfection of sgRNA and Cas9 protein, single-cell colonies were isolated. We confirmed successful knockout by DNA sequencing, supported by the absence of ERα mRNA and protein (Fig. S4B, C). ERα-KO disrupted the expression of clock factors in MCF-7 cells compared to the control (Fig. S4 D, E). In contrast to the robust 24-hour rhythms in control MCF-7 cells, there was a complete loss of circadian BMAL1-Luc rhythms in all four clones of MCF-7 cells with ERα-KO (Fig. S5A). In addition, an ERα selective agonist PPT (Propyl Pyrazole Triol) synchronized circadian clocks in MCF-7 cells in a dose-dependent manner, further supporting a regulatory role of ER signaling in MCF-7 cell circadian function (Fig. S5B).

CYCLOPS 2.0 analysis revealed global changes in rhythmic gene expression patterns and pathways in Luminal A samples

Guided by the experimental and informatic evidence for persistent rhythms in Luminal A tumors and the relative abundance of Luminal A samples in the TCGA database, we next used CYCLOPS 2.0 to order Luminal A tumors (Table S2). There is likely significant non-circadian heterogeneity among Luminal A samples. We projected the Luminal A data onto the eigengene space computed from the non-cancerous samples[36] to emphasize the variation resulting from circadian time. Using the CYCLOPS 2.0 model, we included data from both non-cancerous and Luminal A samples in the ordering, now listing tumor status as a covariate. After ordering and applying cosinor regression to the Luminal A samples, seven core clock genes, including DBP, NR1D1, NR1D2, TEF, PER3, NFIL3, and CRY1, meet the initial criteria for cycling (Fig. 4A, B). At a BHq threshold of 0.05, we identified ~1,100 genes as rhythmic. When we imposed a relative cycling amplitude greater than 1/3, we reduced the number of identified cycling transcripts to ~675 (File. S2). Of course, differences in sample size and non-circadian variability may have contributed to these changes. Thus, in addition to simply identifying genes that meet our statistical cutoffs in Luminal A, we used nested regression models as we[36] and others[54,55] have done previously, to directly test for changes in cycling between Luminal A and non-cancerous samples (File. S3). This nested modeling approach tests the importance of tumor-dependent cycling parameters while accounting for tumor-dependent differences in mean expression level. We observe changes in core clock gene and clock output gene rhythms in Luminal A samples (Fig. 4A, B). For example, while TEF shows decreased amplitude in the Luminal A samples, its partner and structural/functional paralogue[56], DBP, shows increased amplitude. As in the non-cancerous samples, Luminal A samples show "rush hours" of rhythmic transcription (Fig. 4C). However, here, the proportion of samples assigned to the window that precedes the ARNTL (BMAL1) acrophase (inferred early evening) is much higher. Using our nested regression models to compare the fit amplitude for transcripts that cycled in either Luminal A or non-cancerous samples, we find that more transcripts lose as opposed to gain amplitude in Luminal A samples (Fig. 4D). Of note, TCGA includes a limited number of

matched Luminal A tumors and non-cancerous samples from the same patient. The sample phases assigned to the tumors and their non-cancerous matches are poorly correlated (Fig. 4E).

At a gene set level, many pathways demonstrate continued circadian orchestration in the Luminal A samples (Fig. 4F). Phase set enrichment analysis reveals cycling in EMT, androgen responsiveness, and numerous immune and inflammatory pathways. We used two complementary approaches to focus on pathway-level differences in Luminal A and non-cancerous output rhythms. To identify pathways with enhanced rhythmicity in Luminal A, we first ranked the full complement of genes that cycled in either Luminal A or non-cancerous tissue by the log fold change in amplitude. We then used GSEA to identify gene sets enriched for more marked amplitude increases in this ranked list. Alternatively, we used nested regression to identify transcripts that showed statistically significant differential cycling (BHq<0.05) between Luminal A and non-cancerous samples. Focusing on genes with a more than five-fold gain in amplitude in Luminal A samples, we used EnrichR to identify pathways overrepresented in this discrete set. Both methods yield similar results (Fig. 4G, H). EMT and angiogenesis pathways—critical to cell invasion and growth support—show increased cycling in Luminal A samples. We find that adipogenesis appears to have reduced cycling using the same two analyses (Fig. 4I, J). Pathways related to fatty acid metabolism and NFkB signaling (among others) also show reduced cycling in Luminal A tumors using one or the other analysis (Fig. 4I, J).

CYCLOPS magnitude as a measure of global circadian rhythm strength

While we understand the amplitude of a single rhythmic waveform, meaningful, global measures of transcriptional rhythm strength still need to be well established. For example, it is generally unknown if high amplitude circadian expression in some genes predicts high amplitude circadian expression of others. CYCLOPS operates on eigengenes—global descriptors of expression that summarize the behavior of many cycling genes. CYCLOPS projects these data onto a plane where a circular structure is apparent. We use the angular position of any sample on this circle to infer its internal molecular phase. We also calculate the radial distance of each sample from the circle's center. Geometrically, we interpret CYCLOPS magnitude (CMag) (Fig. 5A) as a weighted sum of the amplitudes of the individually cycling seed genes. This concept resembles the PCA plots of cycling gene expression in Brooks et al.[57]. The distribution of CYCLOPS magnitudes obtained from the Luminal A samples is broad with a long tail (Fig. 5B). Dividing samples into equal thirds based on CMag, we find that across all transcripts cycling in Luminal A samples, the amplitude of cycling is generally greater in high magnitude samples as compared to low magnitude samples (Fig. 5C, D). Unlike Luminal A samples as a whole (Fig. 4E), the circadian molecular phases assigned to high CMag Luminal A samples generally match the phases assigned to their non-cancerous pair (Fig. 5E). This suggests that higher CMag in Luminal A samples is indicative of a more robust clock.

Circadian rhythm strength predicts prognosis and modulates metastatic potential

We investigated if rhythm strength influenced tumor biology and prognosis. Patients with Luminal A tumors, as assessed by the PAM50 panel[52], were stratified into three equally sized groups based on the CMag of their tumors (low, medium, and high CMag). Using TCGA outcome data, we evaluated these patients' 5-year survival. Retrospectively, the risk of death increases among patients with high-magnitude Luminal A tumors (Fig. 5F). This difference is statistically significant ($p=0.047$, ANOVA). The increased risk in the high-magnitude tumor group remains statistically significant when we tested its influence in a generalized (logistic regression) model that also included patient age and the presence of known metastases at diagnosis ($p<0.05$). A high-magnitude tumor increased the relative risk by ~1.5x, over and above the risk established by the other covariates. Indeed, the predictive value of tumor magnitude remains significant in a model that includes MKI67 transcript expression ($p<0.05$). Of some note, while the same trend appears examining a broader outcome of death OR new cancer event (Fig. S6), this trend is not statistically significant.

CYCLOPS magnitude is broadly associated with the cycling amplitude of many genes. Given its prognostic importance, we next identified rhythmic pathways that showed the most marked differences in high-magnitude samples. For each transcript that showed statistically significant cycling in Luminal A samples, we compared the amplitude estimated from the high-magnitude samples (top third) to the amplitude estimated from lower-magnitude samples (bottom two-thirds). Again, we leveraged both enrichment and overrepresentation approaches to analyze these results at the pathway level. When we compare high- and lower-magnitude samples, our analyses show that EMT-related genes exhibit the most pronounced changes in cycling (Fig. 5G, H). Given the well-established role of EMT in tumor biology and, in particular, metastatic potential, we hypothesized that high amplitude rhythms might modulate Luminal A tumor cell behavior and the potential for invasion.

Most core circadian clock genes have paralogues that can functionally compensate for molecular knockdown[58]. Only BMAL1 is essential for circadian locomotor function[59]. To establish the role of circadian clocks in regulating breast cancer cell behavior, we used lentiviral shRNA for BMAL1 to disrupt cellular clock functions in rhythmic MCF-7 cells. As expected, the lack of BMAL1 abolished circadian reporter rhythms in MCF-7 cells (Fig. 6A). We used hanging drop and cell invasion assays to evaluate the invasion of MCF-7 cells through a 3D collagen I matrix microenvironment. We assessed invasiveness by measuring the distance from the center of the spheroid (initial droplet) to the edge of the furthest cell. Circadian disruption through BMAL1 deficiency inhibited the rate of cell invasion in both MCF-7 cells ($p< 0.001$, Fig. 6B, C) and primary Luminal A breast tumor cells (Fig. S7A). When we disrupted the molecular clock with KL001, which stabilizes both CRY1/CRY2, we observed a similar suppression of cell invasiveness (Fig. 6D-F). Next, MCF-7 cell proliferation was assessed by expression of Ki-67 and real-time quantitative live cell imaging using IncuCyte. BMAL1 knockdown increased levels of Ki-67 (Fig. S7B) and cell proliferation

($p < 0.0001$) (Fig. S7C, Video. S3) in MCF-7 cells. As such, the loss of molecular clock rhythm in MCF-7 cells compromises breast cancer cell invasion into the 3D matrix, despite increasing cell proliferation.

Discussion

This work used informatic ordering (CYCLOPS 2.0) to integrate newly collected, time-stamped biopsies with public data. We reconstructed temporal rhythms in non-cancerous breast tissue and Luminal A breast tumors. In non-cancerous tissue, our approach reveals the cycling of inflammatory, EMT, and estrogen response pathway genes. Experiments with Luminal A organoids show continued, albeit dampened rhythms. Disrupted rhythms are also evident in our informatic circadian reconstruction of Luminal A tumors. Strikingly, retrospective analysis shows that Luminal A cancer patients with high rhythm strength tumors had increased 5-year mortality. EMT pathway genes show the most marked increase in cycling when comparing tumors with higher and lower rhythm strength. Given the importance of EMT in cell invasion, we hypothesized that tumors with high rhythm strength might show increased metastatic potential. Accordingly, 3D culture experiments using established Luminal A cancer cell lines and primary Luminal A cells show reduced invasion following molecular clock disruption. As such, our study links subtype-specific circadian disruption in breast cancer to EMT, metastatic potential, and prognosis.

A bi-directional web of transcription factors and direct protein-protein interactions couples the cell-intrinsic circadian clocks and the cell cycle. Core circadian clock genes include the likely tumor suppressors PER1 and PER2[60-62]. More recently, researchers have shown that the master clock activators BMAL1 and CLOCK have anti-apoptotic roles, promoting liver cell proliferation through the cell cycle regulator Wee-1[63]. On the other hand, oncogenes such as c-MYC or KRAS interfere with circadian pacemaking[24,25].

The circadian-cancer connection may be vital in breast cancer. Several epidemiologic studies have now linked night shift work with breast cancer risk[26-28]. In mouse models bearing primary mammary tumors or breast cancer xenografts, the efficacies of Doxorubicin and Celecoxib are time-of-day dependent[64,65]. However, the difficulty of obtaining time-course clinical samples across multiple circadian cycles in a large, clinically informative cohort hinders our understanding of circadian biology and its translation in human breast cancer.

Several supervised learning algorithms (e.g., BodyTime, TimeSignature, TimeTable, and ZeitZeiger) predict internal clock time from time-unknown human samples[66-69]. These approaches require “training data” that spans the tissues and conditions covered in later applications. BodyTime, for example, uses a small set of transcriptomic biomarkers from blood monocytes to predict the melatonin phase[67]. These approaches show promise when applied to the specific tissue for which they were trained. However, they

are not designed for application to new tissues or disease states (such as solid tumors) without specific training data.

In contrast, CYCLOPS[36] uses global descriptors of expression structure and unsupervised machine learning that identifies more general signatures of rhythmic processes. CYCLOPS does not require exact knowledge of the particular cycling genes in a tissue or the specific temporal relationship between those rhythmic genes. Instead, CYCLOPS requires a list of "seed genes" likely to cycle in a given tissue. It assumes a fixed relative phase relationship between the cycling seed genes across subjects (e.g., BMAL1 precedes NR1D1 by a relatively fixed amount in the oscillations in each sample). More recently, other unsupervised and semi-supervised approaches have emerged. Most notably, Talamanca et al.[45] aimed to increase the power of this approach, focusing on GTEx data, where many sample tissues were taken from the same individuals. Their approach assumes that tissues obtained from the same individual at the same time are at the same molecular phase.

In our work, however, the limitations of having a single tissue type are compounded by the need to aggregate data from several sources. We specifically tailored our modifications to CYCLOPS for these issues. In this context, non-circadian covariates and batch effects in processing can likely overwhelm circadian variation. As we demonstrate in our benchmarking, batch-correcting approaches like COMBAT that attempt to "normalize away" these differences are unlikely to overcome this obstacle. If different centers have different biases in collection time, that approach may remove much of the circadian signal. This challenge is particularly relevant when combining clinical biopsy and autopsy-based collections. CYCLOPS 2.0 explicitly accommodates these issues, finding batch and covariate adjustments to utilize a common underlying periodic structure for all datasets.

While our CYCLOPS 2.0 ordering of non-cancerous breast tissue is consistent with well-established circadian physiology (i.e., the relative phase relationships between core clock genes) and meets various informatic quality checks, it is always reasonable to question informatic results. We cannot dismiss the influence of non-circadian variability on the ordering process. Our hybrid experimental design lends considerable reassurance. This design required only a small number of newly collected time-stamped samples to guide our efforts and demonstrate that the informatic ordering reflects natural temporal variation. This informatics-guided approach reflects a practical compromise, allowing us to infer molecular rhythms without exhaustive time course sampling more confidently. It should also be noted that CYCLOPS, like other ordering methods, infers time as a function of gene expression. Therefore, using time as an independent variable for cycling analysis is somewhat fraught. We have attempted to address this, as we did previously[36], by implementing a more stringent modified cosinor regression and imposing strict numerical thresholds.

Clock gene correlation analysis from breast cancer samples showed subtype-dependent changes in the core-clock organization, supported by our in vitro data showing subtype-dependent clock functionality in tumor organoids. Both approaches revealed a critical role in estrogen responsiveness in regulating breast cancer clocks. Previous work using microarray data to study the correlation between clock genes in node-negative breast cancer patients supports this concept of breast cancer subtype-dependent clock changes. Pairwise correlations between functionally related clock genes (e.g., PER2-PER3 and CRY2-PER3) were more robust in ER+/HER2- and weaker in ER-/HER2+ tumors[70].

Among breast cancer subtypes, Luminal A tumors had the most robust evidence for persistent rhythms, prompting our interest in ordering these tissues along circadian time. We find marked changes in the informatically reconstructed cycling in Luminal A tumors; many genes and pathways, including chemotherapeutic targets, gained or lost rhythmicity. Using CYCLOPS magnitude as a measure of the global rhythm strength in each sample, we identify marked variations in the rhythm strength of Luminal A tumors. The global magnitude of rhythmic oscillation in Luminal A tumors negatively correlates with five-year mortality and positively correlates with cycling in EMT pathway genes. Our in vitro experimental evidence casually links molecular clock disturbance with cancer cell invasion in a 3D model, thus supporting our informatic result. The work of De et al., who observed MCF-7 cells and noted circadian rhythms in EMT-associated changes in cell morphology[71], also buttresses our results.

Our results also agree with a previous analysis of TCGA data comparing paired tumor and non-tumor samples in 14 cancer types. Specifically, in breast cancer, they report a similar downregulation of PER1, PER2, CRY2, and HLF, while CLOCK, ARNTL(BMAL1), and BHLHE40 levels remained relatively unchanged[72]. However, by including a temporal ordering component in the analysis of Luminal A tumors, we observe changes in rhythmic patterns. For example, we observe that ARNTL(BMAL1) loses rhythmicity in addition to a change in basal expression. Similarly, while HLF cycling shows increased amplitude, its functional paralogue[73] DBP shows decreased cycling amplitude. This data will allow cancer researchers to identify chemotherapeutic targets with temporal properties which differ between cancer and non-cancerous tissue, opening a potential chronotherapeutic opportunity. For example, we note cycling in BRAF and other kinase pathway target genes (File. S4-S8). We hypothesize that highly rhythmic Luminal A tumors, which have the worst prognosis, likely due to increased invasiveness despite the reduced proliferative potential, will also be most responsive to time-aware therapies.

These new insights bring us one step closer to personalized circadian medicine. Our results also underscore vital outstanding questions. Comparing rhythms in non-tumor and luminal A samples, the EMT pathway genes stood out for demonstrating increased cycling in tumor samples. Comparing cycling between Luminal A tumors with high/low global rhythm strength again highlights the EMT pathway. Our repeated identification of EMT as a rhythmically coordinated pathway in Luminal A tumors is particularly

intriguing, given recent reports that the metastatic spread of breast cancer accelerates during sleep[74]. Although our experimental results show that Luminal A tumors have cell-autonomous rhythms, our informatic study design cannot distinguish clinically relevant direct clock outputs from rhythms imparted from cycling hormones or other physiological signals. Tumors with high rhythm magnitudes may be more responsive to host signals. Using mouse models, Hill and colleagues previously identified nocturnal light exposure and the corresponding change in host melatonin rhythms as influencing EMT[75]. While the association between tumor rhythm strength, EMT cycling, and patient prognosis is important regardless of mechanism, distinguishing these possibilities is likely essential for targeted therapy.

Further investigations are needed to evaluate the relative contributions of host and tumor rhythms in modulating human disease. Our experimental results showing a change in tumor invasiveness following clock disruption suggest that tumor-autonomous rhythms causally influence metastatic potential. However, it is also possible that circadian fitness or responsiveness is a marker of other features that contribute to an aggressive phenotype. In addition, we cannot be sure these disrupted tumor rhythms retain a ~24-hour period in vivo. As CYCLOPS does not explicitly measure time but rather an ordering relative to an internal molecular cycle, it is possible that in vivo tumor-autonomous rhythms have a longer or shorter period.

Of particular note, our result suggesting tumor rhythm strength is a potential prognostic marker requires significant follow-up and prospective verification in an independent cohort before any clinical application should be considered. Currently, CYCLOPS uses the complete list of ~70 “seed genes” to compute the magnitude score. A smaller cohort of transcripts could likely suffice for this purpose. While circadian magnitude offers prognostic value beyond PAM50 tumor type and MKI67 levels, we do not have immunostained Ki-67 levels in these TCGA samples. While MKI67 transcript and Ki-67 protein levels correlate, they are clearly different. However, we predict that the mechanistic insights our results suggest and the awareness that high-magnitude tumors are better candidates for circadian medicine approaches may prove most useful.

Our results also emphasize the importance of subtype and patient-specific analysis of tumor rhythms. The interactions between cancer biology and circadian rhythms are multifaceted and tumor dependent. The biological differences between tumor subtypes extend far beyond the clock. Indeed, our screening analysis, like previously noted informatic studies, suggests that more aggressive HER2 and triple-negative tumors have weaker or absent rhythms. Nevertheless, we find that within Luminal A tumors, increasing rhythm strength appears to predict increased invasiveness. We believe it is ill-advised to make blanket statements based on a single tumor type or to compare rhythms in tumor types with vastly different biological features. Our results cannot be applied directly to other tumor types. Future studies could test the intriguing hypothesis that specific cancer cells “hijack” the clock mechanism to temporally organize metabolic programs, evade immune surveillance, suppress apoptosis, or facilitate intravasation and metastasis.

Some cancers may specifically disrupt the circadian check on cell division. Other cancer cells may have evolved to break loose from circadian control altogether to suit their needs best[63,73]. For Luminal A tumors, like most organisms, tumor rhythms may impart increased biological fitness – to the detriment of the patient. Taken as a whole, the biological insights from this study may help lay the groundwork for improved breast cancer prevention (e.g., lifestyle changes), new prognostic biomarkers, and more effective personalized breast cancer treatments.

Acknowledgments

J.A.H., G.W., J.B.H. and R.C.A. were supported by the National Cancer Institute (5R01CA227485). S-Y.L, S.J.H., R.C. and Q-J.M. were supported by the Breast Cancer Now grant (2022FebPR1518). S-Y.L. and Q-J.M. were also supported by the Helen Muir Fund from the Wellcome Centre for Cell-Matrix Research (088785/Z/09). R.C.A. received additional support from 5R01AG068577. J-W.L. was supported by a Medical Research Council PhD Studentship.

We would like to thank the Manchester Cancer Research Centre Biobank for access to clinical breast samples and pathological characterizations. We thank Prof. Charles Streuli for his invaluable inputs and advice with the design of this project. We thank Dr. Dharshika Pathiranage, Miss Xiang-jun Zhao for their kind assistance with various experiments. We also thank the Histology and Bioimaging Core Facilities and the Genome Editing Unit (University of Manchester) for their technical support and advice.

Author contributions

R.C.A., Q-J.M. and J.B.H. conceived the study. Q-J.M., R.C.A., J.B.H., S.J.H. and R.C. secured funding. S-Y.L., J.A.H., G.W, J-W.L. and C.F.G performed experiments. R.C.A., Q-J.M., G.W., S-Y.L. and J.A.H. wrote the manuscript. All authors edited the manuscript. S.J.H., R.C.A. Q-J.M, and A.A. supervised the project and provided expertise, reagents, and feedback.

Declaration of interests

J.B.H. is on the scientific advisory board for Synchronicity Pharma. The remaining authors declare no competing interests.

Tables. 1 Patient demographics for 43 pairs of Manchester human breast samples

Patient ID	Gender	Age	Time of resection	Type	Grade	ER[a]	PR[b]	HER2[c]	Ki-67
W005787	Female	72	17:10	IDC	3	0	0	3	40%
W005805	Female	74	16:35	IDC	2	8	8	1	5%
W005821	Female	62	15:06	IDC	3	0	0	0	70%
W005830	Female	38	16:05	IDC	3	8	5	1	38%
W005831	Female	78	12:55	IMC	3	0	0	0	38%
W005859	Female	44	15:20	IDC	2	8	8	1	14%
W005863	Female	51	16:40	IMC	2	8	5	1	36%
W005925	Female	65	15:50	IDC	3	8	0	3	-
W006024	Female	93	12:45	IDC	3	2	0	0	62%
W006029	Female	54	13:10	ILC	2	8	7	1	25%
W006034	Female	76	13:50	IDC	2	8	8	1	21%
W006044	Female	60	12:30	IDC	2	8	8	1	28%
W006045	Female	63	11:55	IDC	1	0	0	1	82%
W006053	Female	47	16:00	IDC	3	8	8	0	50%
W006055	Female	75	13:50	IDC	3	2	0	1	63%
W006071	Female	45	13:00	IDC	2	7	7	2	27%
W006074	Female	75	16:10	IDC + DCIS	2	8	7	1	17%
W006077	Female	40	10:40	IDC	3	0	0	0	-
W006078	Female	70	16:45	IDC	2	8	0	2	25%
W006140	Female	77	10:25	IAC	2	0	0	1	12%
W006147	Female	73	15:40	IDC	3	0	0	1	30%
W006155	Female	68	11:18	IDC	3	8	3	1	21%
W006161	Female	60	15:55	ILC	2	8	6	2	10%
W006167	Female	85	10:54	IDC	2	8	7	1	30%
W006193	Female	54	13:50	IDC + DCIS	2	8	7	2	36%
W006195	Female	33	11:45	IDC	1	8	7	1	20%
W006212	Female	42	12:55	IDC	2	8	0	3	-
W006217	Female	48	10:45	IDC	2	7	8	2	20%
W006218	Female	76	13:15	IDC	2	8	8	1	12%
W006219	Female	71	12:20	ILC	2	8	4	1	5%
W006226	Female	43	15:00	IDC	3	0	0	3	-
W006238	Female	56	10:05	IDC	3	8	4	2	29%
W006241	Female	80	16:45	IDC	3	8	7	2	35%
W006267	Female	71	17:03	IPLC	3	7	5	1	30%
W006268	Female	41	12:00	ILC	2	7	7	2	19%
W006312	Female	63	15:58	IDC	2	8	7	1	13%
W006314	Female	54	12:15	IDC	2	8	8	1	19%
W006335	Female	45	11:40	IDC	3	8	7	0	10%
W006506	Female	69	15:55	ILC	2	6	0	2	20%
W006510	Female	49	16:20	IDC	3	8	3	0	33%
W006511	Female	53	10:15	IDC	1	8	6	1	25%
W006542	Female	39	13:50	ILC + DCIS	2	8	8	1	10%
W006553	Female	72	14:40	IDC	3	0	0	1	18%

a, estrogen receptor; b, progesterone receptor; c, human epidermal growth factor receptor 2

Reference

Uncategorized References

1. Sung, H., Ferlay, J., Siegel, R.L., Laversanne, M., Soerjomataram, I., Jemal, A., and Bray, F. (2021). Global Cancer Statistics 2020: GLOBOCAN Estimates of Incidence and Mortality Worldwide for 36 Cancers in 185 Countries. CA Cancer J Clin *71*, 209-249. 10.3322/caac.21660.

2. Siegel, R.L., Miller, K.D., Fuchs, H., and Jemal, A. (2021). Cancer Statistics, 2021. CA Cancer J Clin *71*, 7- 33. https://doi.org/10.3322/caac.21654.

3. Trayes, K.P., and Cokenakes, S.E.H. (2021). Breast Cancer Treatment. Am Fam Physician *104*, 171-178.

4. Kesson, E.M., Allardice, G.M., George, W.D., Burns, H.J., and Morrison, D.S. (2012). Effects of multidisciplinary team working on breast cancer survival: retrospective, comparative, interventional cohort study of 13 722 women. BMJ *344*. 10.1136/bmj.e2718.

5. Global Burden of Disease 2019 Cancer Collaboration. Cancer Incidence, Mortality, Years of Life Lost, Years Lived With Disability, and Disability-Adjusted Life Years for 29 Cancer Groups From 2010 to 2019: A Systematic Analysis for the Global Burden of Disease Study 2019. (2022). JAMA Oncol. *8*, 420–444. doi:10.1001/jamaoncol.2021.6987.

6. Park, J., Rodriguez, J.L., O'Brien, K.M., Nichols, H.B., Hodgson, M.E., Weinberg, C.R., and Sandler, D.P. (2021). Health-related quality of life outcomes among breast cancer survivors. Cancer *127*, 1114-1125. https://doi.org/10.1002/cncr.33348.

7. Williams, A.M., Khan, C.P., Heckler, C.E., Barton, D.L., Ontko, M., Geer, J., Kleckner, A.S., Dakhil, S., Mitchell, J., Mustian, K.M., et al. (2021). Fatigue, anxiety, and quality of life in breast cancer patients compared to non-cancer controls: a nationwide longitudinal analysis. Breast Cancer Research and Treatment *187*, 275–285. https://doi.org/10.1007/s10549-020-06067-6.

8. Battisti, N.M.L., Reed, M.W.R., Herbert, E., Morgan, J.L., Collins, K.A., Ward, S.E., Holmes, G.R., Bradburn, M., Walters, S.J., Burton, M., et al. (2021). Bridging the Age Gap in breast cancer: Impact of chemotherapy on quality of life in older women with early breast cancer. European Journal of Cancer *144*, 269-280. https://doi.org/10.1016/j.ejca.2020.11.022.

9. Chakradhar, S. (2018). About time. Nat Med *24*, 696-698. 10.1038/s41591-018-0069-8.

10. Sulli, G., Manoogian, E.N.C., Taub, P.R., and Panda, S. (2018). Training the Circadian Clock, Clocking the Drugs, and Drugging the Clock to Prevent, Manage, and Treat Chronic Diseases. Trends Pharmacol Sci *39*, 812-827. 10.1016/j.tips.2018.07.003.

11. Cederroth, C.R., Albrecht, U., Bass, J., Brown, S.A., Dyhrfjeld-Johnsen, J., Gachon, F., Green, C.B., Hastings, M.H., Helfrich-Förster, C., Hogenesch, J.B., et al. (2019). Medicine in the Fourth Dimension. Cell Metabolism *30*, 238-250. https://doi.org/10.1016/j.cmet.2019.06.019.

12. Sancar, A., and Van Gelder, R.N. (2021). Clocks, cancer, and chronochemotherapy. Science *371*. 10.1126/science.abb0738.

13. Partch, C.L., Green, C.B., and Takahashi, J.S. (2014). Molecular architecture of the mammalian circadian clock. Trends in cell biology *24*, 90-99. 10.1016/j.tcb.2013.07.002.

14. Dibner, C., Schibler, U., and Albrecht, U. (2010). The mammalian circadian timing system: organization and coordination of central and peripheral clocks. Annu Rev Physiol *72*, 517-549. 10.1146/annurev-physiol-021909-135821.

15. Bass, J., and Lazar, M.A. (2016). Circadian time signatures of fitness and disease. Science *354*, 994-999. 10.1126/science.aah4965.

16. Zhang, R., Lahens, N.F., Ballance, H.I., Hughes, M.E., and Hogenesch, J.B. (2014). A circadian gene expression atlas in mammals: implications for biology and medicine. Proc Natl Acad Sci U S A *111*, 16219-16224. 10.1073/pnas.1408886111.

17. Johnson, C.H. (2010). Circadian clocks and cell division: what's the pacemaker? Cell Cycle *9*, 3864-3873. 10.4161/cc.9.19.13205.

18. Masri, S., Cervantes, M., and Sassone-Corsi, P. (2013). The circadian clock and cell cycle: interconnected biological circuits. Curr Opin Cell Biol *25*, 730-734. 10.1016/j.ceb.2013.07.013.

19. Zhang, E.E., Liu, A.C., Hirota, T., Miraglia, L.J., Welch, G., Pongsawakul, P.Y., Liu, X., Atwood, A., Huss, J.W., 3rd, Janes, J., et al. (2009). A genome-wide RNAi screen for modifiers of the circadian clock in human cells. Cell *139*, 199-210. 10.1016/j.cell.2009.08.031.

20. Altman, B.J., Hsieh, A.L., Sengupta, A., Krishnanaiah, S.Y., Stine, Z.E., Walton, Z.E., Gouw, A.M., Venkataraman, A., Li, B., Goraksha-Hicks, P., et al. (2015). MYC Disrupts the Circadian Clock and Metabolism in Cancer Cells. Cell Metab *22*, 1009-1019. 10.1016/j.cmet.2015.09.003.

21. Altman, B.J., Hsieh, A.L., Gouw, A.M., and Dang, C.V. (2017). Correspondence: Oncogenic MYC persistently upregulates the molecular clock component REV-ERBα. Nature Communications *8*, 14862. 10.1038/ncomms14862.

22. Huber, A.-L., Papp, S.J., Chan, A.B., Henriksson, E., Jordan, S.D., Kriebs, A., Nguyen, M., Wallace, M., Li, Z., Metallo, C.M., and Lamia, K.A. (2016). CRY2 and FBXL3 Cooperatively Degrade c-MYC. Mol Cell *64*, 774-789. 10.1016/j.molcel.2016.10.012.

23. Liu, Z., Selby, C.P., Yang, Y., Lindsey-Boltz, L.A., Cao, X., Eynullazada, K., and Sancar, A. (2020). Circadian regulation of c-MYC in mice. Proceedings of the National Academy of Sciences *117*, 21609-21617. doi:10.1073/pnas.2011225117.

24. Pariollaud, M., Ibrahim, L.H., Irizarry, E., Mello, R.M., Chan, A.B., Altman, B.J., Shaw, R.J., Bollong, M.J., Wiseman, R.L., and Lamia, K.A. (2022). Circadian disruption enhances HSF1 signaling and tumorigenesis in Kras-driven lung cancer. Science Advances *8*, eabo1123. doi:10.1126/sciadv.abo1123.

25. Relógio, A., Thomas, P., Medina-Pérez, P., Reischl, S., Bervoets, S., Gloc, E., Riemer, P., Mang-Fatehi, S., Maier, B., Schäfer, R., et al. (2014). Ras-Mediated Deregulation of the Circadian Clock in Cancer. PLOS Genetics *10*, e1004338. 10.1371/journal.pgen.1004338.

26. Van Dycke, K.C., Rodenburg, W., van Oostrom, C.T., van Kerkhof, L.W., Pennings, J.L., Roenneberg, T., van Steeg, H., and van der Horst, G.T. (2015). Chronically Alternating Light Cycles Increase Breast Cancer Risk in Mice. Curr Biol *25*, 1932-1937. 10.1016/j.cub.2015.06.012.

27. Cordina-Duverger, E., Menegaux, F., Popa, A., Rabstein, S., Harth, V., Pesch, B., Brüning, T., Fritschi, L., Glass, D.C., Heyworth, J.S., et al. (2018). Night shift work and breast cancer: a pooled analysis of population-based case-control studies with complete work history. Eur J Epidemiol *33*, 369-379. 10.1007/s10654-018-0368-x.

28. EM, W. (2019). Carcinogenicity of night shift work. Lancet Oncol *20*, 1058-1059. 10.1016/s1470-2045(19)30455-3.

29. Yang, N., Williams, J., Pekovic-Vaughan, V., Wang, P., Olabi, S., McConnell, J., Gossan, N., Hughes, A., Cheung, J., Streuli, C.H., and Meng, Q.J. (2017). Cellular mechano-environment regulates the mammary circadian clock. Nat Commun *8*, 14287. 10.1038/ncomms14287.

30. Blakeman, V., Williams, J.L., Meng, Q.J., and Streuli, C.H. (2016). Circadian clocks and breast cancer. Breast Cancer Res *18*, 89. 10.1186/s13058-016-0743-z.

31. Williams, J., Yang, N., Wood, A., Zindy, E., Meng, Q.J., and Streuli, C.H. (2018). Epithelial and stromal circadian clocks are inversely regulated by their mechano-matrix environment. J Cell Sci *131*. 10.1242/jcs.208223.

32. Broadberry, E., McConnell, J., Williams, J., Yang, N., Zindy, E., Leek, A., Waddington, R., Joseph, L., Howe, M., Meng, Q.J., and Streuli, C.H. (2018). Disrupted circadian clocks and altered tissue mechanics in primary human breast tumours. Breast Cancer Res *20*, 125. 10.1186/s13058-018-1053-4.

33. Hadadi, E., Taylor, W., Li, X.-M., Aslan, Y., Villote, M., Rivière, J., Duvallet, G., Auriau, C., Dulong, S., Raymond-Letron, I., et al. (2020). Chronic circadian disruption modulates breast cancer stemness and immune microenvironment to drive metastasis in mice. Nature Communications *11*, 3193. 10.1038/s41467-020-16890-6.

34. Halberg, F., Cornélissen, G., Ulmer, W., Blank, M., Hrushesky, W., Wood, P., Singh, R.K., and Wang, Z. (2006). Cancer chronomics III. Chronomics for cancer, aging, melatonin and experimental therapeutics researchers. J Exp Ther Oncol *6*, 73-84.

35. Lévi, F., Okyar, A., Dulong, S., Innominato, P.F., and Clairambault, J. (2010). Circadian timing in cancer treatments. Annu Rev Pharmacol Toxicol *50*, 377-421. 10.1146/annurev.pharmtox.48.113006.094626.

36. Anafi, R.C., Francey, L.J., Hogenesch, J.B., and Kim, J. (2017). CYCLOPS reveals human transcriptional rhythms in health and disease. Proceedings of the National Academy of Sciences *114*, 5312-5317. doi:10.1073/pnas.1619320114.

37. Ruben, M.D., Wu, G., Smith, D.F., Schmidt, R.E., Francey, L.J., Lee, Y.Y., Anafi, R.C., and Hogenesch, J.B. (2018). A database of tissue-specific rhythmically expressed human genes has potential applications in circadian medicine. Sci Transl Med *10*. 10.1126/scitranslmed.aat8806.

38. Wu, G., Ruben, M.D., Schmidt, R.E., Francey, L.J., Smith, D.F., Anafi, R.C., Hughey, J.J., Tasseff, R., Sherrill, J.D., Oblong, J.E., et al. (2018). Population-level rhythms in human skin with implications for circadian medicine. Proc Natl Acad Sci U S A *115*, 12313-12318. 10.1073/pnas.1809442115.

39. Weinstein, J.N., Collisson, E.A., Mills, G.B., Shaw, K.R., Ozenberger, B.A., Ellrott, K., Shmulevich, I., Sander, C., and Stuart, J.M. (2013). The Cancer Genome Atlas Pan-Cancer analysis project. Nat Genet *45*, 1113-1120. 10.1038/ng.2764.

40. Lonsdale, J., Thomas, J., Salvatore, M., Phillips, R., Lo, E., Shad, S., Hasz, R., Walters, G., Garcia, F., Young, N., et al. (2013). The Genotype-Tissue Expression (GTEx) project. Nature Genetics *45*, 580-585. 10.1038/ng.2653.

41. Wu, G., Ruben, M.D., Francey, L.J., Smith, D.F., Sherrill, J.D., Oblong, J.E., Mills, K.J., and Hogenesch, J.B. (2020). A population-based gene expression signature of molecular clock phase from a single epidermal sample. Genome Medicine *12*, 73. 10.1186/s13073-020-00768-9.

42. Shilts, J., Chen, G., and Hughey, J.J. (2018). Evidence for widespread dysregulation of circadian clock progression in human cancer. PeerJ *6*, e4327. 10.7717/peerj.4327.

43. Hollis, H.C., Francis, J.N., and Anafi, R.C. (2022). Multi-tissue transcriptional changes and core circadian clock disruption following intensive care. Front Physiol *13*, 942704. 10.3389/fphys.2022.942704.

44. Cornelissen, G. (2014). Cosinor-based rhythmometry. Theoretical Biology and Medical Modelling *11*, 16. 10.1186/1742-4682-11-16.

45. Talamanca, L., Gobet, C., and Naef, F. (2023). Sex-dimorphic and age-dependent organization of 24-hour gene expression rhythms in humans. Science *379*, 478-483. 10.1126/science.add0846.

46. Zhang, R., Podtelezhnikov, A.A., Hogenesch, J.B., and Anafi, R.C. (2016). Discovering Biology in Periodic Data through Phase Set Enrichment Analysis (PSEA). Journal of Biological Rhythms *31*, 244-257. 10.1177/0748730416631895.

47. Subramanian, A., Tamayo, P., Mootha, V.K., Mukherjee, S., Ebert, B.L., Gillette, M.A., Paulovich, A., Pomeroy, S.L., Golub, T.R., Lander, E.S., and Mesirov, J.P. (2005). Gene set enrichment analysis: A knowledge-based approach for interpreting genome-wide expression profiles. Proceedings of the National Academy of Sciences *102*, 15545-15550. doi:10.1073/pnas.0506580102.

48. Chen, E.Y., Tan, C.M., Kou, Y., Duan, Q., Wang, Z., Meirelles, G.V., Clark, N.R., and Ma'ayan, A. (2013). Enrichr: interactive and collaborative HTML5 gene list enrichment analysis tool. BMC Bioinformatics *14*, 128. 10.1186/1471-2105-14-128.

49. Kuleshov, M.V., Jones, M.R., Rouillard, A.D., Fernandez, N.F., Duan, Q., Wang, Z., Koplev, S., Jenkins, S.L., Jagodnik, K.M., Lachmann, A., et al. (2016). Enrichr: a comprehensive gene set enrichment analysis web server 2016 update. Nucleic Acids Res *44*, W90-97. 10.1093/nar/gkw377.

50. Xie, Z., Bailey, A., Kuleshov, M.V., Clarke, D.J.B., Evangelista, J.E., Jenkins, S.L., Lachmann, A., Wojciechowicz, M.L., Kropiwnicki, E., Jagodnik, K.M., et al. (2021). Gene Set Knowledge Discovery with Enrichr. Curr Protoc *1*, e90. 10.1002/cpz1.90.

51. van 't Veer, L.J., Dai, H., van de Vijver, M.J., He, Y.D., Hart, A.A.M., Mao, M., Peterse, H.L., van der Kooy, K., Marton, M.J., Witteveen, A.T., et al. (2002). Gene expression profiling predicts clinical outcome of breast cancer. Nature *415*, 530-536. 10.1038/415530a.

52. Netanely, D., Avraham, A., Ben-Baruch, A., Evron, E., and Shamir, R. (2016). Expression and methylation patterns partition luminal-A breast tumors into distinct prognostic subgroups. Breast Cancer Research *18*, 74. 10.1186/s13058-016-0724-2.

53. Jensen, C., and Teng, Y. (2020). Is It Time to Start Transitioning From 2D to 3D Cell Culture? Front Mol Biosci *7*, 33. 10.3389/fmolb.2020.00033.

54. Pelikan, A., Herzel, H., Kramer, A., and Ananthasubramaniam, B. (2022). Venn diagram analysis overestimates the extent of circadian rhythm reprogramming. Febs j *289*, 6605-6621. 10.1111/febs.16095.

55. Singer, J.M., and Hughey, J.J. (2019). LimoRhyde: A Flexible Approach for Differential Analysis of Rhythmic Transcriptome Data. J Biol Rhythms *34*, 5-18. 10.1177/0748730418813785.

56. Gachon, F., Olela, F.F., Schaad, O., Descombes, P., and Schibler, U. (2006). The circadian PAR-domain basic leucine zipper transcription factors DBP, TEF, and HLF modulate basal and inducible xenobiotic detoxification. Cell Metabolism *Volume 4*, 25-36. https://doi.org/10.1016/j.cmet.2006.04.015.

57. Brooks, T.G., Mrčela, A., Lahens, N.F., Paschos, G.K., Grosser, T., Skarke, C., FitzGerald, G.A., and Grant, G.R. (2022). Nitecap: An Exploratory Circadian Analysis Web Application. J Biol Rhythms *37*, 43-52. 10.1177/07487304211054408.

58. Baggs, J.E., Price, T.S., DiTacchio, L., Panda, S., FitzGerald, G.A., and Hogenesch, J.B. (2009). Network Features of the Mammalian Circadian Clock. PLOS Biology *7*, e1000052. 10.1371/journal.pbio.1000052.

59. Bunger, M.K., Wilsbacher, L.D., Moran, S.M., Clendenin, C., Radcliffe, L.A., Hogenesch, J.B., Simon, M.C., Takahashi, J.S., and Bradfield, C.A. (2000). Mop3 Is an Essential Component of the Master Circadian Pacemaker in Mammals. Cell *103*, 1009–1017. https://doi.org/10.1016/S0092-8674(00)00205-1.

60. Fu, L., Pelicano, H., Liu, J., Huang, P., and Lee, C. (2002). The circadian gene Period2 plays an important role in tumor suppression and DNA damage response in vivo. Cell *111*, 41-50. 10.1016/s0092-8674(02)00961-3.

61. Gery, S., Komatsu, N., Baldjyan, L., Yu, A., Koo, D., and Koeffler, H.P. (2006). The circadian gene per1 plays an important role in cell growth and DNA damage control in human cancer cells. Mol Cell *22*, 375-382. 10.1016/j.molcel.2006.03.038.

62. Gotoh, T., Kim, J.K., Liu, J., Vila-Caballer, M., Stauffer, P.E., Tyson, J.J., and Finkielstein, C.V. (2016). Model-driven experimental approach reveals the complex regulatory distribution of p53 by the circadian factor Period 2. Proceedings of the National Academy of Sciences *113*, 13516-13521. doi:10.1073/pnas.1607984113.

63. Qu, M., Zhang, G., Qu, H., Vu, A., Wu, R., Tsukamoto, H., Jia, Z., Huang, W., Lenz, H.-J., Rich, J.N., and Kay, S.A. (2023). Circadian regulator BMAL1::CLOCK promotes cell proliferation in hepatocellular carcinoma by controlling apoptosis and cell cycle. Proceedings of the National Academy of Sciences *120*, e2214829120. doi:10.1073/pnas.2214829120.

64. Blumenthal, R.D., Waskewich, C., Goldenberg, D.M., Lew, W., Flefleh, C., and Burton, J. (2001). Chronotherapy and chronotoxicity of the cyclooxygenase-2 inhibitor, celecoxib, in athymic mice bearing human breast cancer xenografts. Clin Cancer Res *7*, 3178-3185.

65. Granda, T.G., Filipski, E., D'Attino, R.M., Vrignaud, P., Anjo, A., Bissery, M.C., and Lévi, F. (2001). Experimental chronotherapy of mouse mammary adenocarcinoma MA13/C with docetaxel and doxorubicin as single agents and in combination. Cancer Res *61*, 1996-2001.

66. Hughey, J.J. (2017). Machine learning identifies a compact gene set for monitoring the circadian clock in human blood. Genome Med *9*, 19. 10.1186/s13073-017-0406-4.

67. Wittenbrink, N., Ananthasubramaniam, B., Munch, M., Koller, B., Maier, B., Weschke, C., Bes, F., de Zeeuw, J., Nowozin, C., Wahnschaffe, A., et al. (2018). High-accuracy determination of internal circadian time from a single blood sample. J Clin Invest *128*, 3826-3839. 10.1172/JCI120874.

68. Braun, R., Kath, W.L., Iwanaszko, M., Kula-Eversole, E., Abbott, S.M., Reid, K.J., Zee, P.C., and Allada, R. (2018). Universal method for robust detection of circadian state from gene expression. Proceedings of the National Academy of Sciences *115*, E9247-E9256. doi:10.1073/pnas.1800314115.

69. Laing, E.E., Möller-Levet, C.S., Poh, N., Santhi, N., Archer, S.N., and Dijk, D.-J. (2017). Blood transcriptome based biomarkers for human circadian phase. eLife *6*, e20214. 10.7554/eLife.20214.

70. Cadenas, C., van de Sandt, L., Edlund, K., Lohr, M., Hellwig, B., Marchan, R., Schmidt, M., Rahnenfuhrer, J., Oster, H., and Hengstler, J.G. (2014). Loss of circadian clock gene expression is associated with tumor progression in breast cancer. Cell Cycle *13*, 3282-3291. 10.4161/15384101.2014.954454.

71. De, A., Beligala, D.H., Sharma, V.P., Burgos, C.A., Lee, A.M., and Geusz, M.E. (2020). Cancer stem cell generation during epithelial-mesenchymal transition is temporally gated by intrinsic circadian clocks. Clinical & Experimental Metastasis *37*, 617-635. 10.1007/s10585-020-10051-1.

72. Ye, Y., Xiang, Y., Ozguc, F.M., Kim, Y., Liu, C.-J., Park, P.K., Hu, Q., Diao, L., Lou, Y., Lin, C., et al. (2018). The Genomic Landscape and Pharmacogenomic Interactions of Clock Genes in Cancer Chronotherapy. Cell Systems *6*, 314-328.e312. https://doi.org/10.1016/j.cels.2018.01.013.

73. Alamoudi, A.A. (2021). Why do cancer cells break from host circadian rhythm? Insights from unicellular organisms. BioEssays *43*, 2000205. https://doi.org/10.1002/bies.202000205.

74. Diamantopoulou, Z., Castro-Giner, F., Schwab, F.D., Foerster, C., Saini, M., Budinjas, S., Strittmatter, K., Krol, I., Seifert, B., Heinzelmann-Schwarz, V., et al. (2022). The metastatic spread of breast cancer accelerates during sleep. Nature *607*, 156-162. 10.1038/s41586-022-04875-y.

75. Mao, L., Dauchy, R.T., Blask, D.E., Slakey, L.M., Xiang, S., Yuan, L., Dauchy, E.M., Shan, B., Brainard, G.C., Hanifin, J.P., et al. (2012). Circadian Gating of Epithelial-to-Mesenchymal Transition in

Breast Cancer Cells Via Melatonin- Regulation of GSK3beta. Molecular Endocrinology *26*, 1808–1820. 10.1210/me.2012-1071.

76. Chen, C.-Y., Logan, R.W., Ma, T., Lewis, D.A., Tseng, G.C., Sibille, E., and McClung, C.A. (2016). Effects of aging on circadian patterns of gene expression in the human prefrontal cortex. Proceedings of the National Academy of Sciences *113*, 206-211. doi:10.1073/pnas.1508249112.

77. Bossé, Y., Postma, D.S., Sin, D.D., Lamontagne, M., Couture, C., Gaudreault, N., Joubert, P., Wong, V., Elliott, M., van den Berge, M., et al. (2012). Molecular signature of smoking in human lung tissues. Cancer Res *72*, 3753-3763. 10.1158/0008-5472.Can-12-1160.

78. Dobin, A., Davis, C.A., Schlesinger, F., Drenkow, J., Zaleski, C., Jha, S., Batut, P., Chaisson, M., and Gingeras, T.R. (2013). STAR: ultrafast universal RNA-seq aligner. Bioinformatics *29*, 15-21. 10.1093/bioinformatics/bts635.

79. Li, B., and Dewey, C.N. (2011). RSEM: accurate transcript quantification from RNA-Seq data with or without a reference genome. BMC Bioinformatics *12*, 323. 10.1186/1471-2105-12-323.

80. Bezanson, J., Edelman, A., Karpinski, S., and Shah, V.B. (2017). Julia: A Fresh Approach to Numerical Computing. SIAM Review *59*, 65-98. 10.1137/141000671.

81. Innes, M. (2018). Flux: Elegant machine learning with Julia. J. Open Source Softw. *3*, 602.

82. Leek, J.T., Johnson, W.E., Parker, H.S., Jaffe, A.E., and Storey, J.D. (2012). The sva package for removing batch effects and other unwanted variation in high-throughput experiments. Bioinformatics *28*, 882-883. 10.1093/bioinformatics/bts034.

Key resources table

REAGENT or RESOURCE	SOURCE	IDENTIFIER
Antibodies		
Alexa Fluor™ 488 Phalloidin	Thermo Scientific	Cat# R37110
Anti-Rabbit BMAL1	Homemade (Weaver Lab)	N/A
Anti-Rabbit Cytokeratin 8	Abcam	Cat# ab53280 RRID: AB_860091
Anti-Rabbit CLOCK	Proteintech	Cat# 18094-1-AP RRID: AB_2878497
Anti-Rabbit CRY1	Proteintech	Cat# 13474-1-AP RRID: AB_10697652
Anti-Rabbit ERα	Cell Signaling Technology	Cat# 8644 RRID: AB_2617128
Anti-Rabbit HER2	Cell Signaling Technology	Cat# 2165 RRID: AB_10692490
Anti-Rabbit Ki-67	Abcam	Cat# ab16667 RRID: AB_302459
Anti-Rabbit PER2	Abclonal	Cat# a5107 RRID: 2863447
Anti-Rabbit Vimentin	Abcam	Cat# ab92547 RRID: AB_10562134
Primers		
Bacterial and virus strains		
NEB Stable Competent E. coli (High efficiency)	New England Biolabs	Cat# C3040H
Biological samples		
Human breast samples	MCRC Biobank	Ref: 21_QIME_01
TCGA-BRCA samples	FireBrowse	http://firebrowse.org/
GTEx v8 breast samples	GTEX portal[40]	https://storage.googleapis.com/gtex_analysis_v8/rna_seq_data/GTEx_Analysis_2017-06-05_v8_RNASeQCv1.1.9_gene_tpm.gct.gz
BA11 brain samples	NIH GEO: GSE71620	Chen et al.[76]
Groningen and Laval lung samples	NIH GEO: GSE23546	Bossé et al.[77]
Chemicals, peptides, and recombinant proteins		
1X Trypsin-EDTA solution	Sigma-Aldrich	Cat# T3924
10X Tris/Glycine/SDS	Bio-Rad	Cat# 1610732
A83-01	Tocirs	Cat# 2939
Acetic Acid Glacial	Fisher scientific	Cat# 10171460
Advanced DMEM/F12	Gibco	Cat# 12634010
Agarose	Bioline	Cat# BIO-41025
Alt-R S.p.Cas9 Nuclease V3	Integrated DNA Technologies	Cat# 1081058
Ampicillin	Sigma-Aldrich	Cat# A9393

B27 supplement (50X), serum free	Gibco	Cat# 17504044
BSA (Bovine Serum Albumins)	Sigma-Aldrich	Cat# A2153
Calcium Chloride	Fisher scientific	Cat# 10171800
Collagenase A	Roche	Cat# 10103186001
Chloroform, 99.8+%	Fisher scientific	Cat# 10784143
Dexamethasone	Sigma-Aldrich	Cat# D4902
Dispase II	Roche	Cat# 37045800
Donkey Serum	Sigma-Aldrich	Cat# D9663
DPX Mountant for histology	Sigma-Aldrich	Cat# 06522
DPBS (1X)	Sigma-Aldrich	Cat# D5652
DMEM/F12 without phenol red	Gibco	Cat# 2063394
Dnase I	Roche	Cat# 11284932001
Dnase-free RNase set	QIAGEN	Cat# 79254
Eosin-Y	Sigma-Aldrich	Cat# E4009
EGF (Epidermal Growth Factor)	Peprotech	Cat# AF-100-15
Ethanol, 99.8+%	Fisher scientific	Cat# 12337163
FBS	Sigma-Aldrich	Cat# 12103C
FGF2 (Fibroblast Growth Factor 2)	Peprotech	Cat# 100-18B
FGF7	Peprotech	Cat# 100-19
FGF10	Peprotech	Cat# 100-26
Gentamicin solution	Sigma-Aldrich	Cat# G1272
GlutaMax 100X	Gibco	Cat# 15630-056
Goat Serum	Sigma-Aldrich	Cat# G9023
Halt™ Protease inhibitor cocktails	Thermo Scientific	Cat# 78429
HBSS	Sigma-Aldrich	Cat# H9394
HCl (Hydrochloric Acid)	Fisher scientific	Cat# 10053023
Hematoxylin Solution, Gill No. 2	Sigma-Aldrich	Cat# GHS216
HEPES	Sigma-Aldrich	Cat# H0887
High-Capacity RNA to cDNA kit	Applied Biosystems	Cat# 4387406
Hyaluronidases	Sigma-Aldrich	Cat# H3885
Hydrogen peroxide solution	Sigma-Aldrich	Cat# 95321
ISOLATE II Genomic DNA kit	Bioline	Cat# BIO-52066
Isopropanol	Fisher scientific	Cat# 10477070
L-Glutamine	Sigma-Aldrich	Cat# G7513
Lipofectamine CRISPRMAX Transfection Regent	Thermo Scientific	Cat# CMAX00015
Beetle Luciferin, Potassium Salt	Promega	Cat# E1603
Lysing Matrix A	MP Biomedicals	Cat# 116910050
Corning Matrigel® Growth Factor Reduced (GFR) Basement Membrane Matrix, LDEV-free	Corning	Cat# 354230
Methanol	Fisher scientific	Cat# 10141720
Methylcellulose	Sigma-Aldrich	Cat# M7027
4-20% Mini-PROTEIN TGX Precast Protein Gels	Bio-Rad	Cat# 4561093
N-Acetylcysteine	Sigma-Aldrich	Cat# A9165
Nicotinamide	Sigma-Aldrich	Cat# N6036
Noggin	Peprotech	Cat# 120-10C

Opti-MEM™ I Reduced Serum Medium, no phenol red	Thermo Scientific	Cat# 11058021
P/S (Penicillin/Streptomycin)	Sigma-Aldrich	Cat# P4333
Polybrene	Sigma-Aldrich	Cat# TR-1003-G
Paraformaldehyde	Sigma-Aldrich	Cat# 95321
Pierce™ BCA Protein Assay Reagent A	Thermo Scientific	Cat# 23223
Pierce™ BCA Protein Assay Reagent B	Thermo Scientific	Cat# 23224
Primocin	Invivogen	Cat# Ant-pm-1
PureCol EZ gel solution	Sigma-Aldrich	Cat# 5074
QIAfilter Plasmid Maxi Kit	QIAGEN	Cat# 12245
QIAquick Gel Extraction Kit	QIAGEN	Cat# 28704
Qubit™ RNA XR Assay Kit	Thermo Scientific	Cat# Q33224
R-spondin 3	Peprotech	Cat# 120-44
RIPA Buffer	Sigma-Aldrich	Cat# R2078
RNAlater™ Stabilization Solution	Thermo Scientific	Cat# AM7020
RNA ScreenTape	Agilent	Cat# 5067-5576
RNA ScreenTape Sample Buffer	Agilent	Cat# 5067-5577
Rneasy Lipid Tissue Mini Kit	QIAGEN	Cat# 74804
SB202190	Sigma-Aldrich	Cat# S7067
SIGMAFAST™ 3,3′-Diaminobenzidine tablets	Sigma-Aldrich	Cat# D4168
Sodium Butyrate	Sigma-Aldrich	Cat# B5887
Sodium citrate (100X)	Abcam	Cat# ab93678
Streptavidin, Peroxidase (Concentrate, for IHC)	Vector	Cat# SA-5004-1
TAE Buffer (50X)	Thermo Scientific	Cat# B49
Takyon ROX probe Mastermix DTTP blue	Eurogenetic	Cat# EUK212
Trans-Blot Tuobo RTA Mini 0.2 μm Nitrocellulose Transfer Kit, for 40 bolts	Bio-Rad	Cat# 1704270
Triton X-100	Thermo Scientific	Cat# 85111
Tween™ 20	Thermo Scientific	Cat# 85113
Xylenes	Fisher scientific	Cat# 15618420
Software and algorithms		
STAR(version 2.5)	Dobin et al.[78]	https://github.com/alexdobin/STAR/releases
RSEM(version 1.3.0)	Li et al.[79]	https://github.com/deweylab/RSEM/releases
R (v4.2.1)	-	https://www.R-project.org
CCMapp	Wu et al.[38]	https://github.com/gangwug/CCMapp
BioRender	-	https://www.biorender.com
Julia (v1.6)	Bezanson et al.[80]	https://doi.org/10.1137/141000671
GSEA (v4.2.3)	Subramanian et al.[47]	https://doi.org/10.1073/pnas.0506580102
PSEA	Zhang et al.[46]	https://doi.org/10.1177/0748730416631895
enrichR.R (v3.1)	Chen et al.[48]	https://doi.org/10.1093/nar/gkw377
Dataframes.jl (v1.3.4)	-	https://dataframes.juliadata.org/stable/

Statistics.jl	-	https://docs.julialang.org/en/v1/stdlib/Statistics/
StatsBase.jl (v0.33.21)	-	https://juliastats.org/StatsBase.jl/stable/
LinearAlgebra.jl	-	https://docs.julialang.org/en/v1/stdlib/LinearAlgebra/
MultivariateStats.jl (v0.10.0)	-	https://juliapackages.com/p/multivariatestats
Flux.jl (v0.13.5)	Innes.[81]	https://doi.org/10.21105/joss.00602
PyPlot.jl (v2.11.0)	-	https://github.com/JuliaPlots/Plots.jl
Distributed.jl	-	https://docs.julialang.org/en/v1/stdlib/Distributed/#
Random.jl	-	https://docs.julialang.org/en/v1/stdlib/Random/
CSV.jl (v0.10.4)	-	https://csv.juliadata.org/stable/
Revise.jl (v3.4.0)	-	https://timholy.github.io/Revise.jl/stable/
Dates.jl	-	https://docs.julialang.org/en/v1/stdlib/Dates/
Multipletesting.jl (v0.5.1)	-	https://zenodo.org/badge/latestdoi/27935122
sva.R (v3.44.0)	Leek et al.[82]	https://doi.org/doi:10.18129/B9.bioc.sva
refGenome (v1.7.7)	-	https://cran.r-project.org/src/contrib/Archive/refGenome/
RTCGA.clinical (20151101.20.0)	-	https://bioconductor.org/packages/release/data/experiment/html/RTCGA.clinical.html
RTCGA (1.20.0)	-	https://www.bioconductor.org/packages/release/bioc/html/RTCGA.html
tidyverse.R (v1.3.2)	-	https://doi.org/10.21105/joss.01686
aod.R (v1.3.2)	-	https://cran.r-project.org/package=aod
circular.R (v0.4-95)	-	https://r-forge.r-project.org/projects/circular/
Other		

Fig. 1

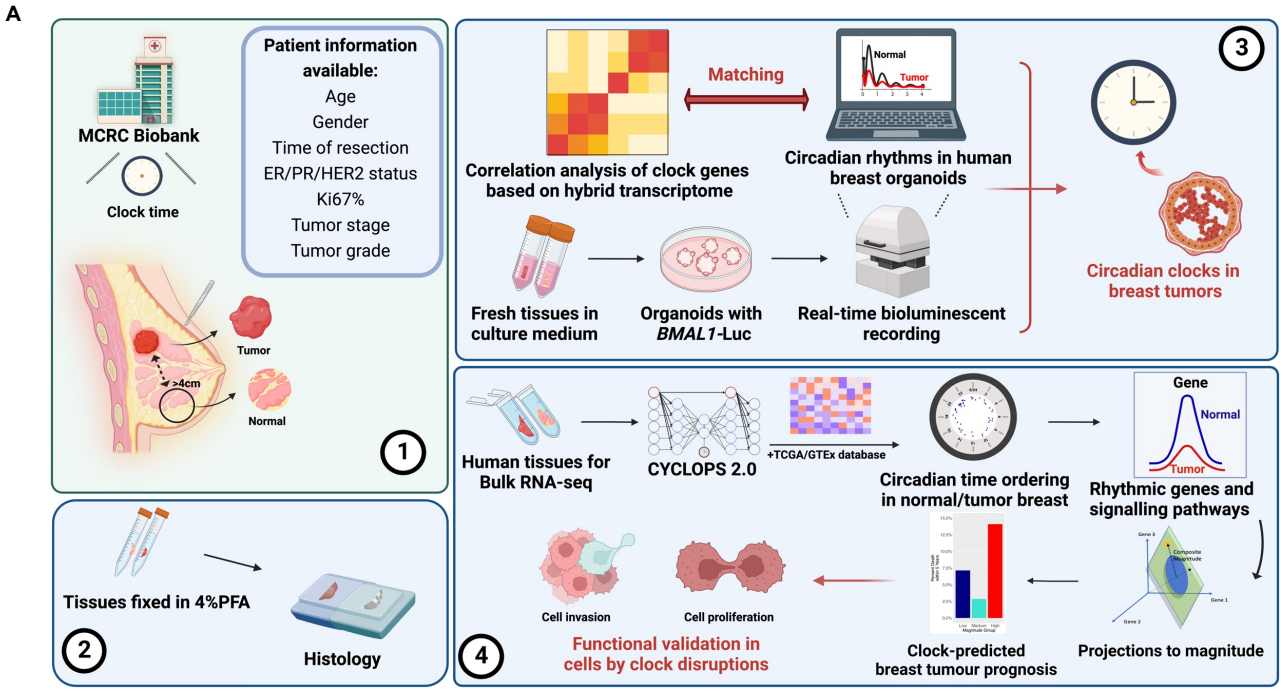
A
MCRC Biobank
Clock time
Patient information available:
Age
Gender
Time of resection
ER/PR/HER2 status
Ki67%
Tumor stage
Tumor grade
Tumor
>4cm
Normal
1
Tissues fixed in 4%PFA
Histology
2
Correlation analysis of clock genes based on hybrid transcriptome
Matching
Normal
Tumor
Circadian rhythms in human breast organoids
3
Circadian clocks in breast tumors
Fresh tissues in culture medium
Organoids with BMAL1-Luc
Real-time bioluminescent recording
Human tissues for Bulk RNA-seq
CYCLOPS 2.0
+TCGA/GTEx database
Circadian time ordering in normal/tumor breast
Gene
Normal
Tumor
Rhythmic genes and signalling pathways
Cell invasion
Cell proliferation
Functional validation in cells by clock disruptions
4
Clock-predicted breast tumour prognosis
Projections to magnitude

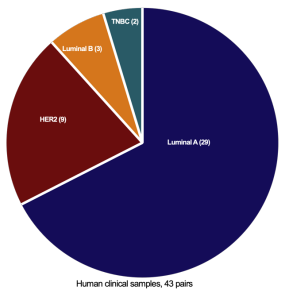
B
TNBC (2)
Luminal B (3)
HER2 (9)
Luminal A (29)
Human clinical samples, 43 pairs

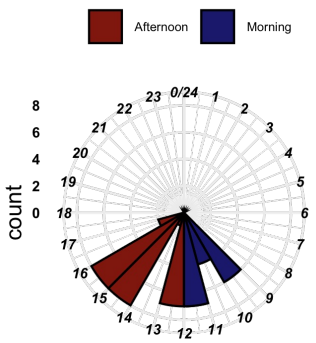
C
Afternoon
Morning
count
0/24
1
2
3
4
5
6
7
8
9
10
11
12
13
14
15
16
17
18
19
20
21
22
23

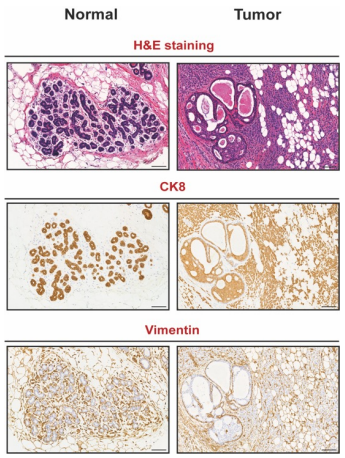
D
Normal
Tumor
H&E staining
CK8
Vimentin

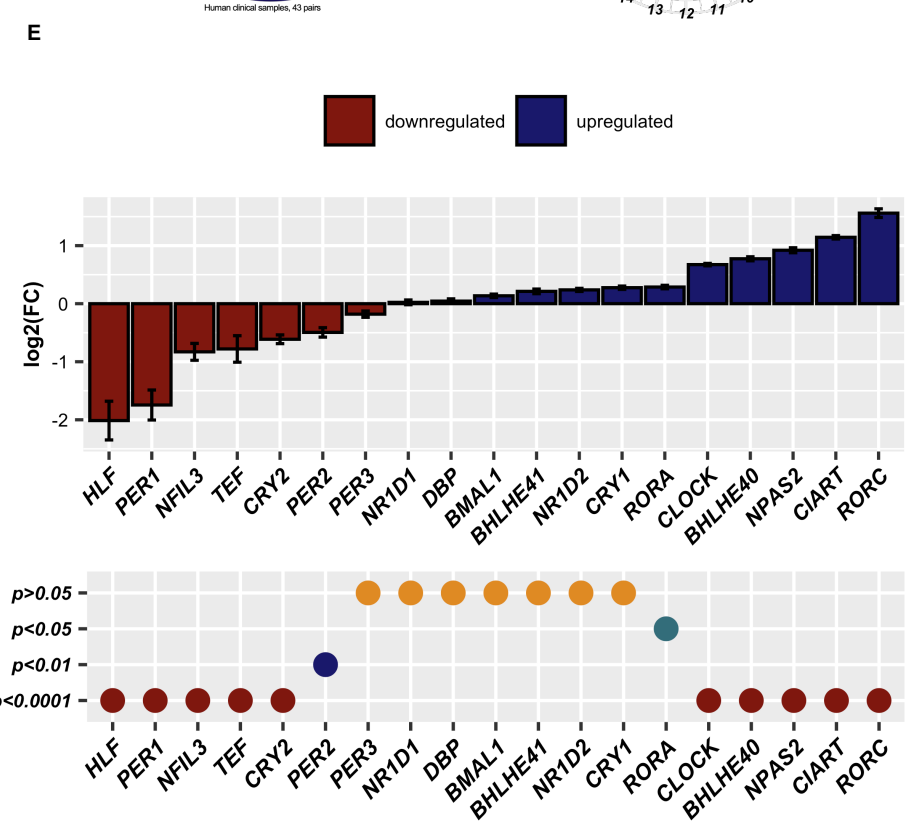
E
downregulated
upregulated
log2(FC)
1
0
-1
-2
HLF
PER1
NFIL3
TEF
CRY2
PER2
PER3
NR1D1
DBP
BMAL1
BHLHE41
NR1D2
CRY1
RORA
CLOCK
BHLHE40
NPAS2
CIART
RORC
p>0.05
p<0.05
p<0.01
p<0.0001

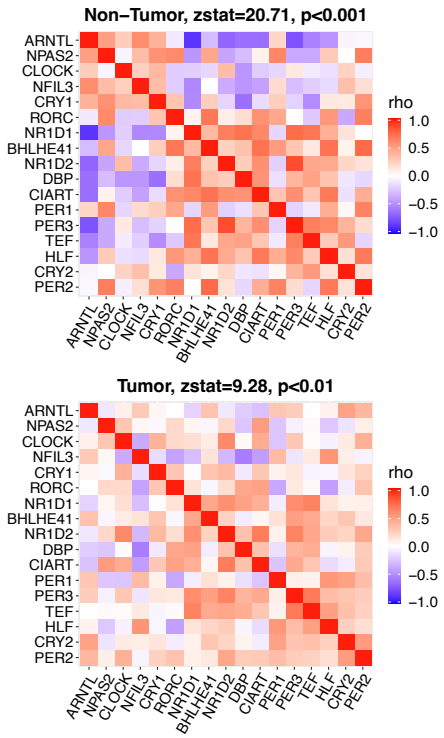
F
Non−Tumor, zstat=20.71, p<0.001
Tumor, zstat=9.28, p<0.01
rho
1.0
0.5
0.0
−0.5
−1.0
ARNTL
NPAS2
CLOCK
NFIL3
CRY1
RORC
NR1D1
BHLHE41
NR1D2
DBP
CIART
PER1
PER3
TEF
HLF
CRY2
PER2

Fig. 2

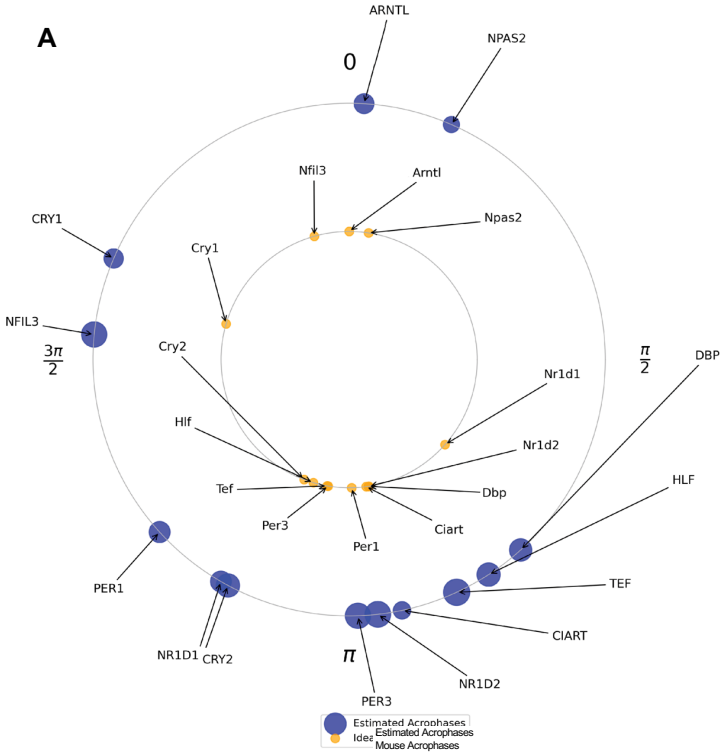

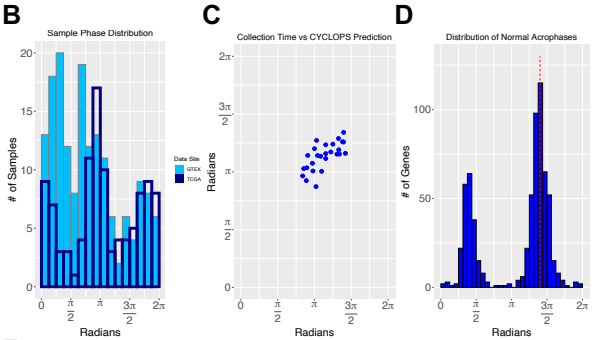

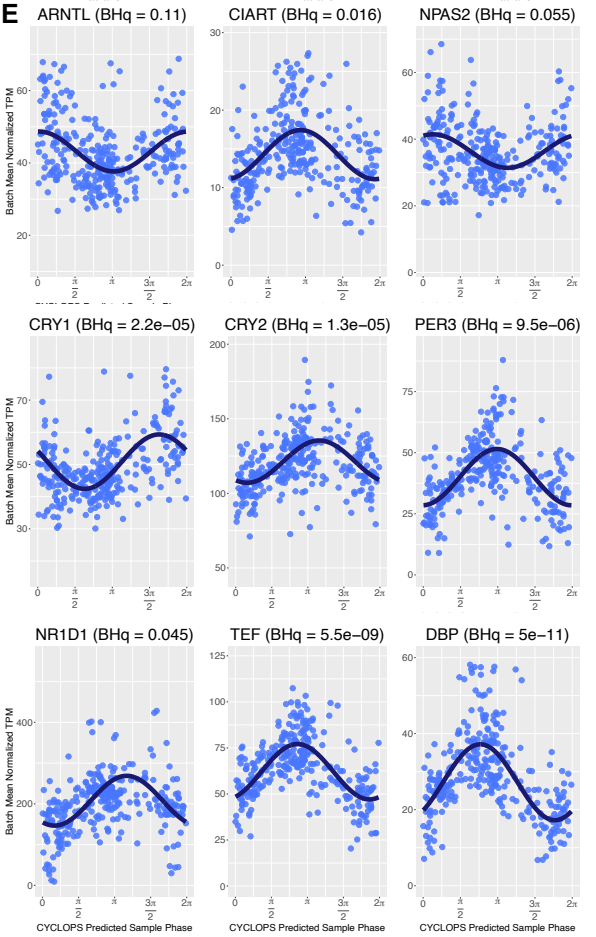

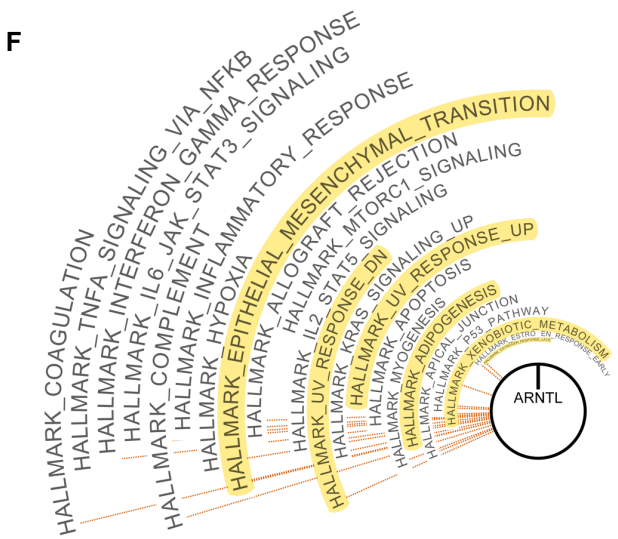

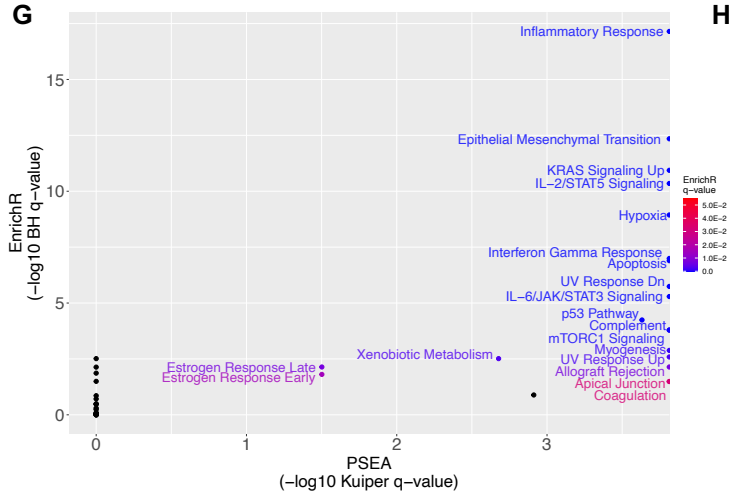

H

Hallmark Gene Set	Classic FDR Q Value
HALLMARK_TNFA_SIGNALING_VIA_NFKB	0E+00
HALLMARK_EPITHELIAL_MESENCHYMAL_TRANSITION	0E+00
HALLMARK_INFLAMMATORY_RESPONSE	2E-04
HALLMARK_UV_RESPONSE_DN	3E-04
HALLMARK_TGF_BETA_SIGNALING	4E-04
HALLMARK_HYPOXIA	3E-03
HALLMARK_MYOGENESIS	4E-03
HALLMARK_KRAS_SIGNALING_UP	2E-02
HALLMARK_IL6_JAK_STAT3_SIGNALING	3E-02
HALLMARK_COAGULATION	5E-02
HALLMARK_APOPTOSIS	5E-02
HALLMARK_MYC_TARGETS_V1	6E-02
HALLMARK_KRAS_SIGNALING_DN	9E-02

Fig. 3

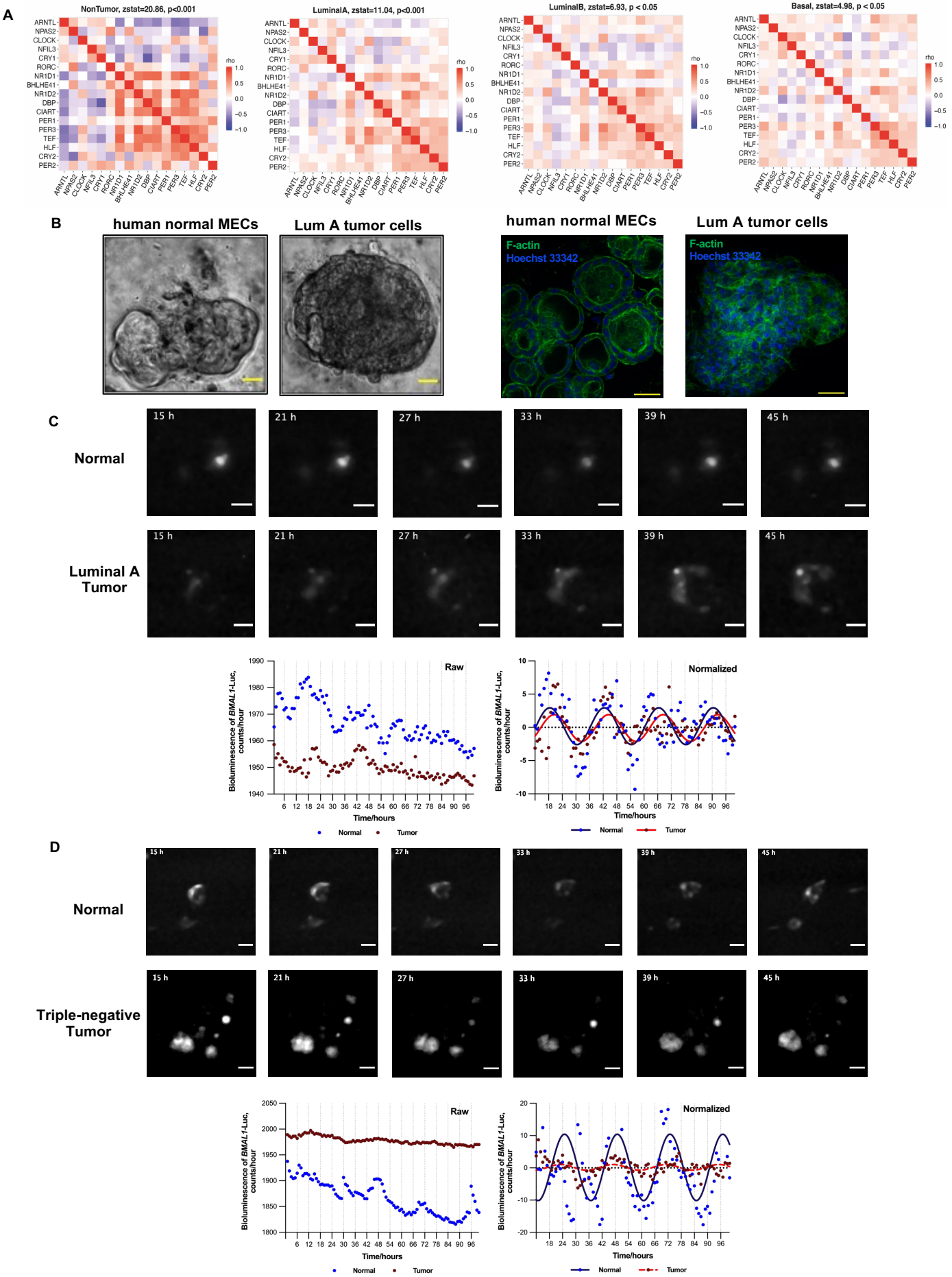
A
NonTumor, zstat=20.86, p<0.001
LuminalA, zstat=11.04, p<0.001
LuminalB, zstat=6.93, p < 0.05
Basal, zstat=4.98, p < 0.05
ARNTL
NPAS2
CLOCK
NFIL3
CRY1
RORC
NR1D1
BHLHE41
NR1D2
DBP
CIART
PER1
PER3
TEF
HLF
CRY2
PER2
rho
1.0
0.5
0.0
−0.5
−1.0
B
human normal MECs
Lum A tumor cells
human normal MECs
Lum A tumor cells
F-actin
Hoechst 33342
C
Normal
Luminal A Tumor
15 h
21 h
27 h
33 h
39 h
45 h
Raw
Normalized
Bioluminescence of BMAL1-Luc, counts/hour
Time/hours
Normal
Tumor
D
Normal
Triple-negative Tumor

Fig. 4

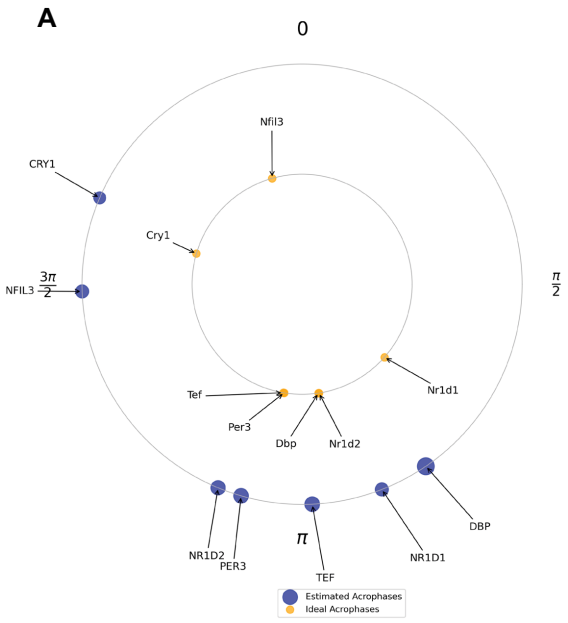

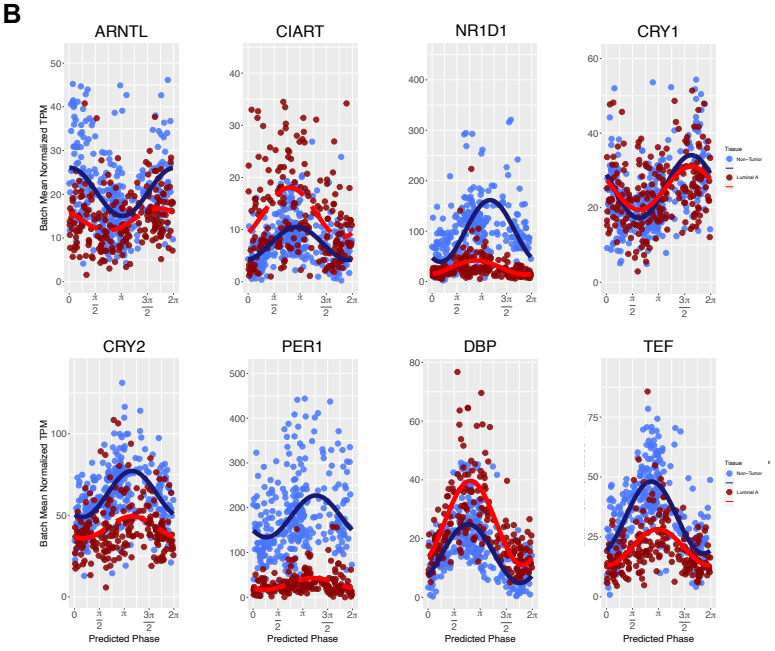

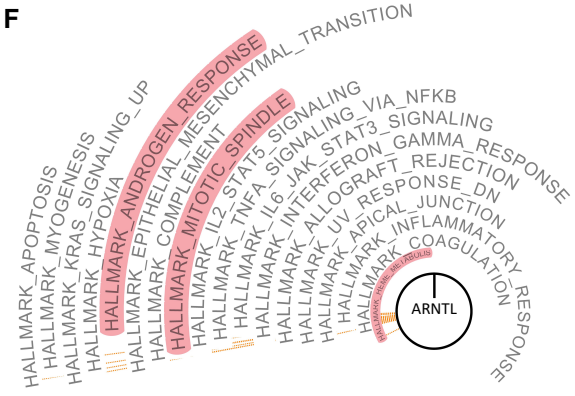

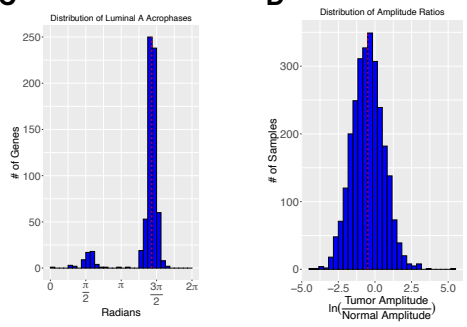

G

Increased Amplitude in Luminal A Hallmark Gene Set	Classic FDR Q Value
HALLMARK_E2F_TARGETS	4E-02
HALLMARK_ALLOGRAFT_REJECTION	5E-02
HALLMARK_EPITHELIAL_MESENCHYMAL_TRANSITION	7E-02
HALLMARK_ANGIOGENESIS	9E-02

H

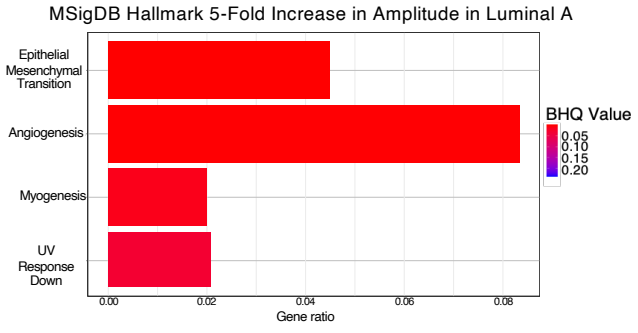

I

Decreased Amplitude in Luminal A Hallmark Gene Set	Classic FDR Q Value
HALLMARK_TNFA_SIGNALING_VIA_NFKB	0E+00
HALLMARK_ADIPOGENESIS	2E-03
HALLMARK_UV_RESPONSE_DN	2E-02

J

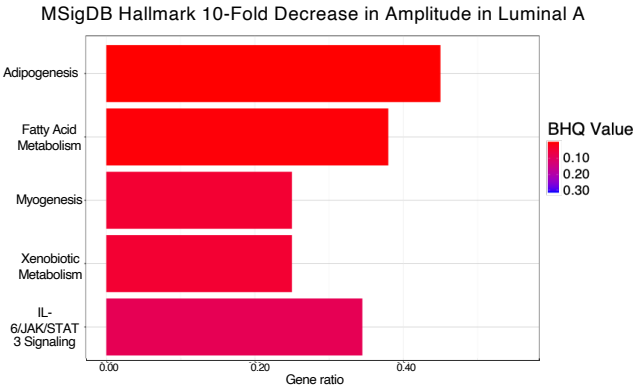

Fig 5

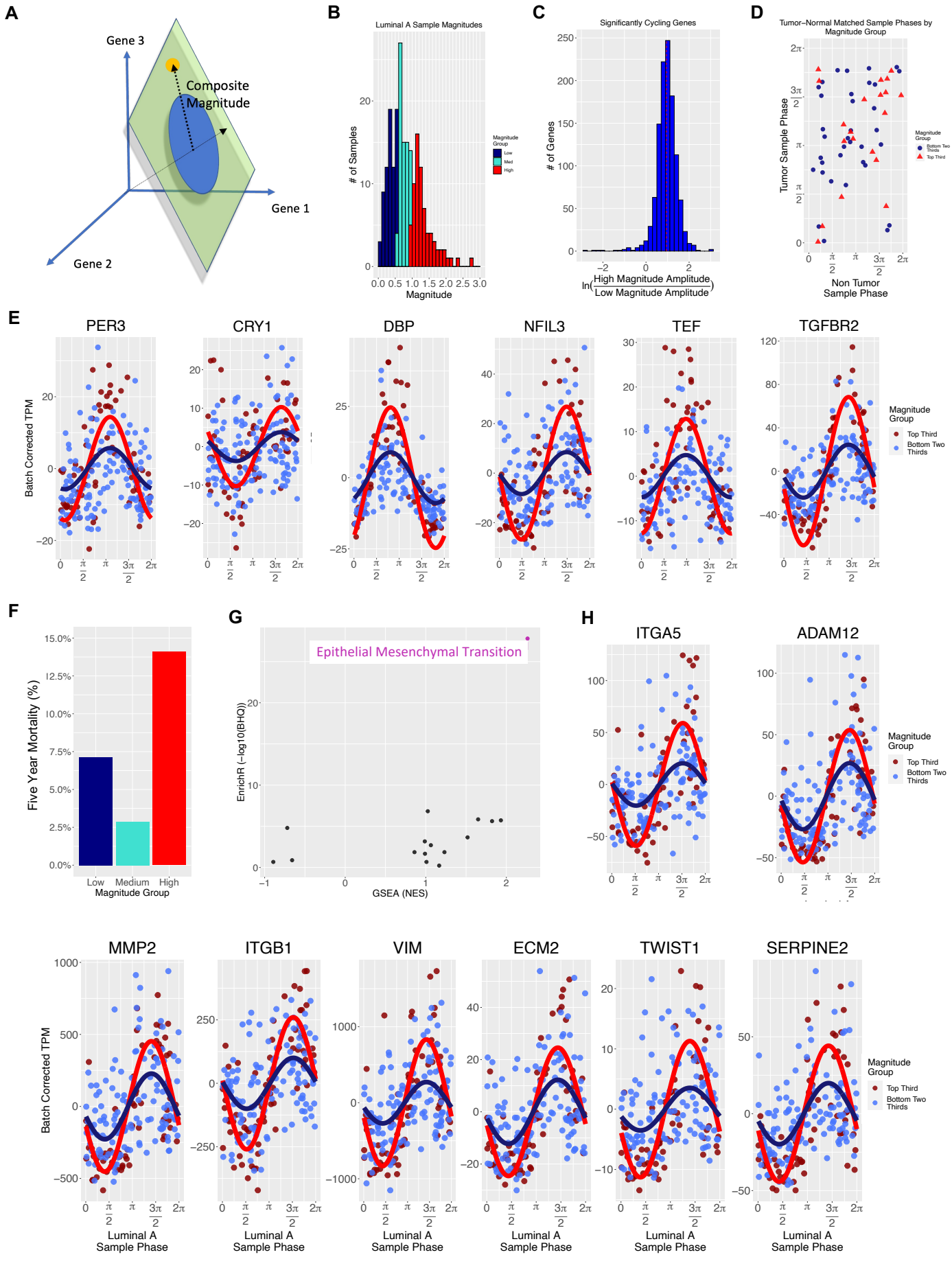
A
Gene 3
Composite Magnitude
Gene 1
Gene 2
B
Luminal A Sample Magnitudes
# of Samples
Magnitude
Magnitude Group
Low
Med
High
C
Significantly Cycling Genes
# of Genes
ln(High Magnitude Amplitude / Low Magnitude Amplitude)
D
Tumor–Normal Matched Sample Phases by Magnitude Group
Tumor Sample Phase
Non Tumor Sample Phase
Magnitude Group
Bottom Two Thirds
Top Third
E
PER3
CRY1
DBP
NFIL3
TEF
TGFBR2
Batch Corrected TPM
Magnitude Group
Top Third
Bottom Two Thirds
F
Five Year Mortality (%)
Low
Medium
High
Magnitude Group
G
Epithelial Mesenchymal Transition
EnrichR (−log10(BHQ))
GSEA (NES)
H
ITGA5
ADAM12
MMP2
ITGB1
VIM
ECM2
TWIST1
SERPINE2
Luminal A Sample Phase

Fig. 6

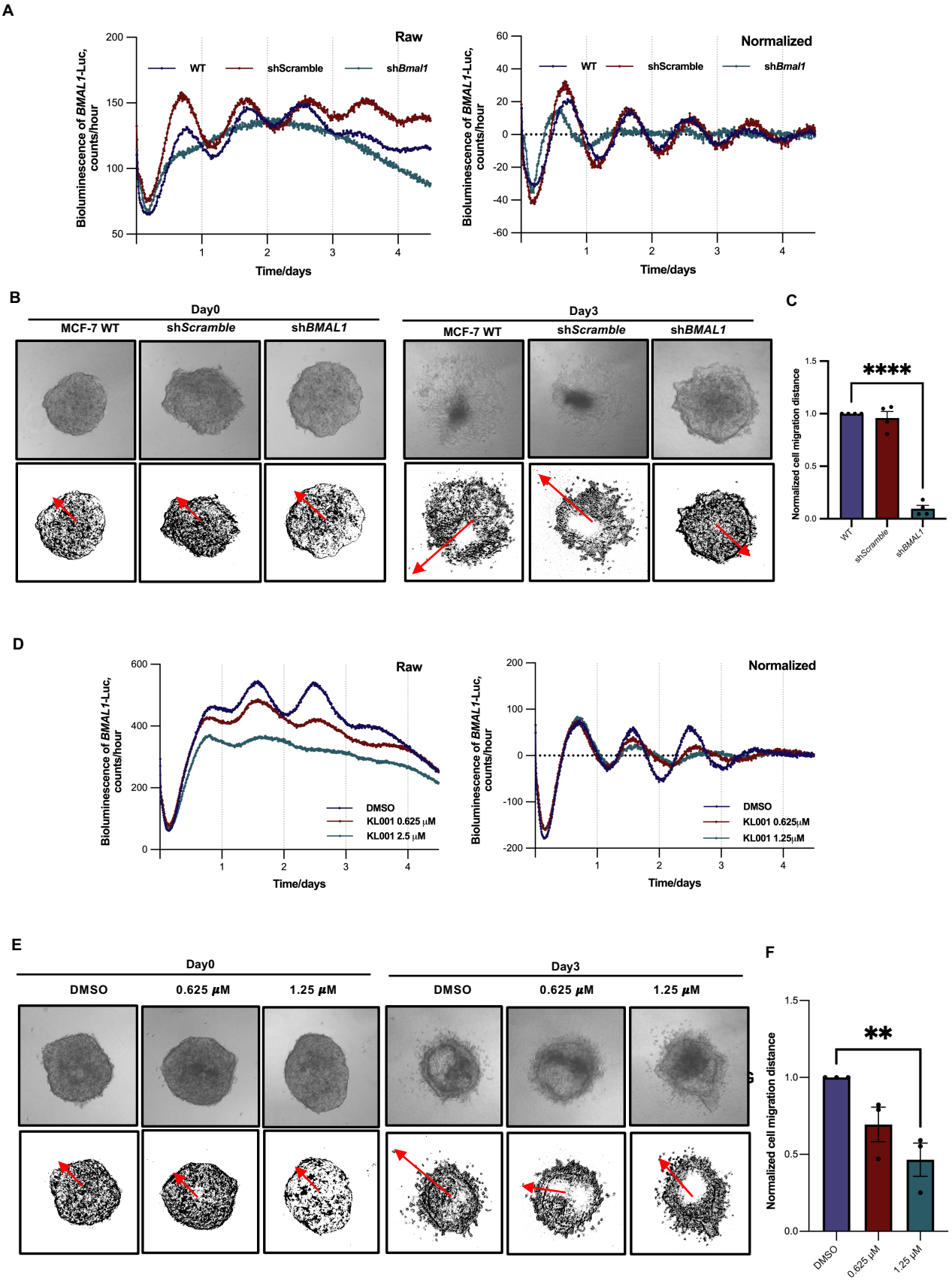
A
Raw
Normalized
WT
shScramble
shBmal1
Bioluminescence of BMAL1-Luc, counts/hour
Time/days
B
Day0
Day3
MCF-7 WT
shScramble
shBMAL1
C
Normalized cell migration distance
****
WT
shScramble
shBMAL1
D
Raw
Normalized
DMSO
KL001 0.625 μM
KL001 2.5 μM
KL001 1.25μM
E
DMSO
0.625 μM
1.25 μM
F
**

Fig. S1

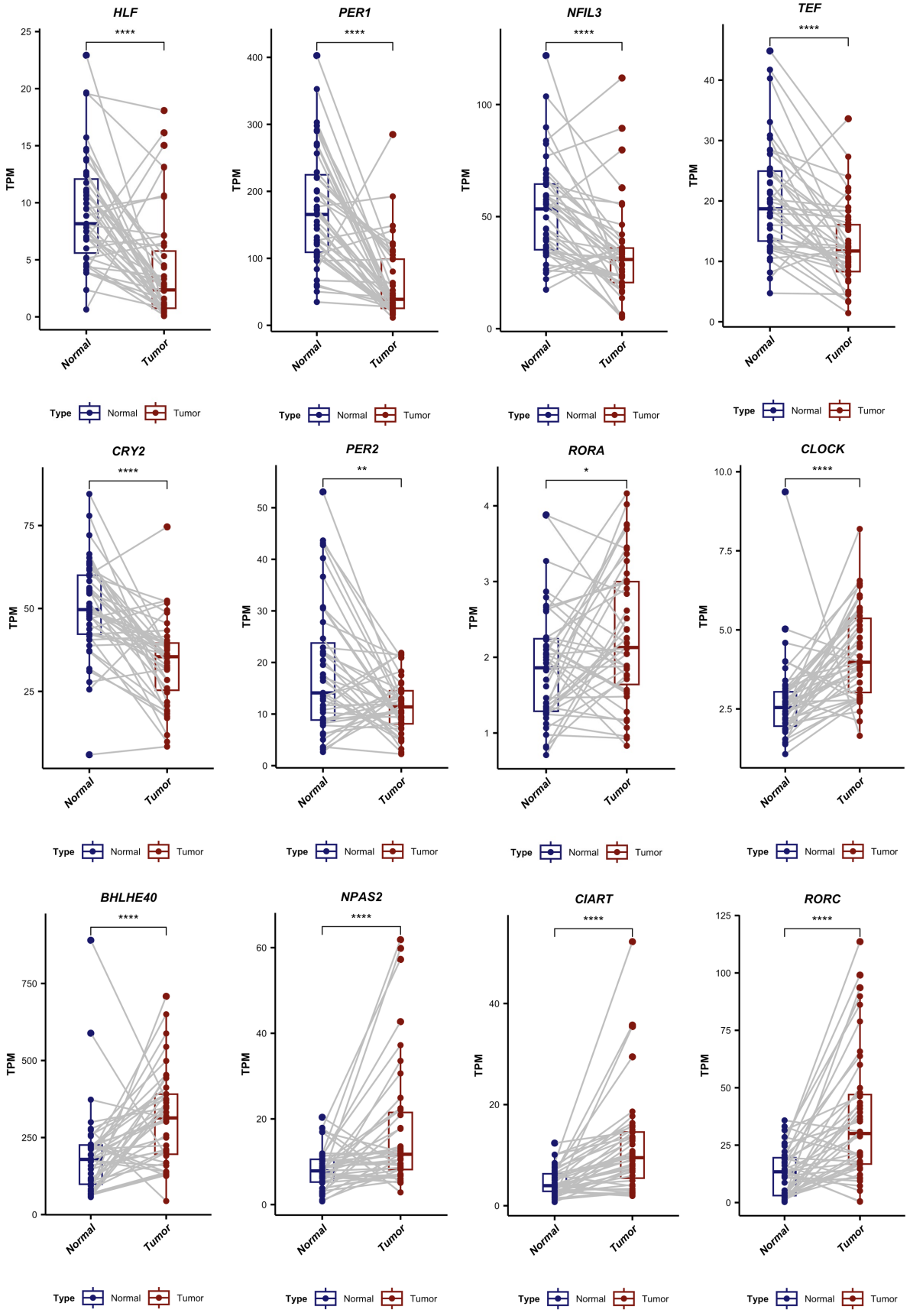
HLF
PER1
NFIL3
TEF
CRY2
PER2
RORA
CLOCK
BHLHE40
NPAS2
CIART
RORC
TPM
Normal
Tumor
Type
****
**
*

Fig. S2

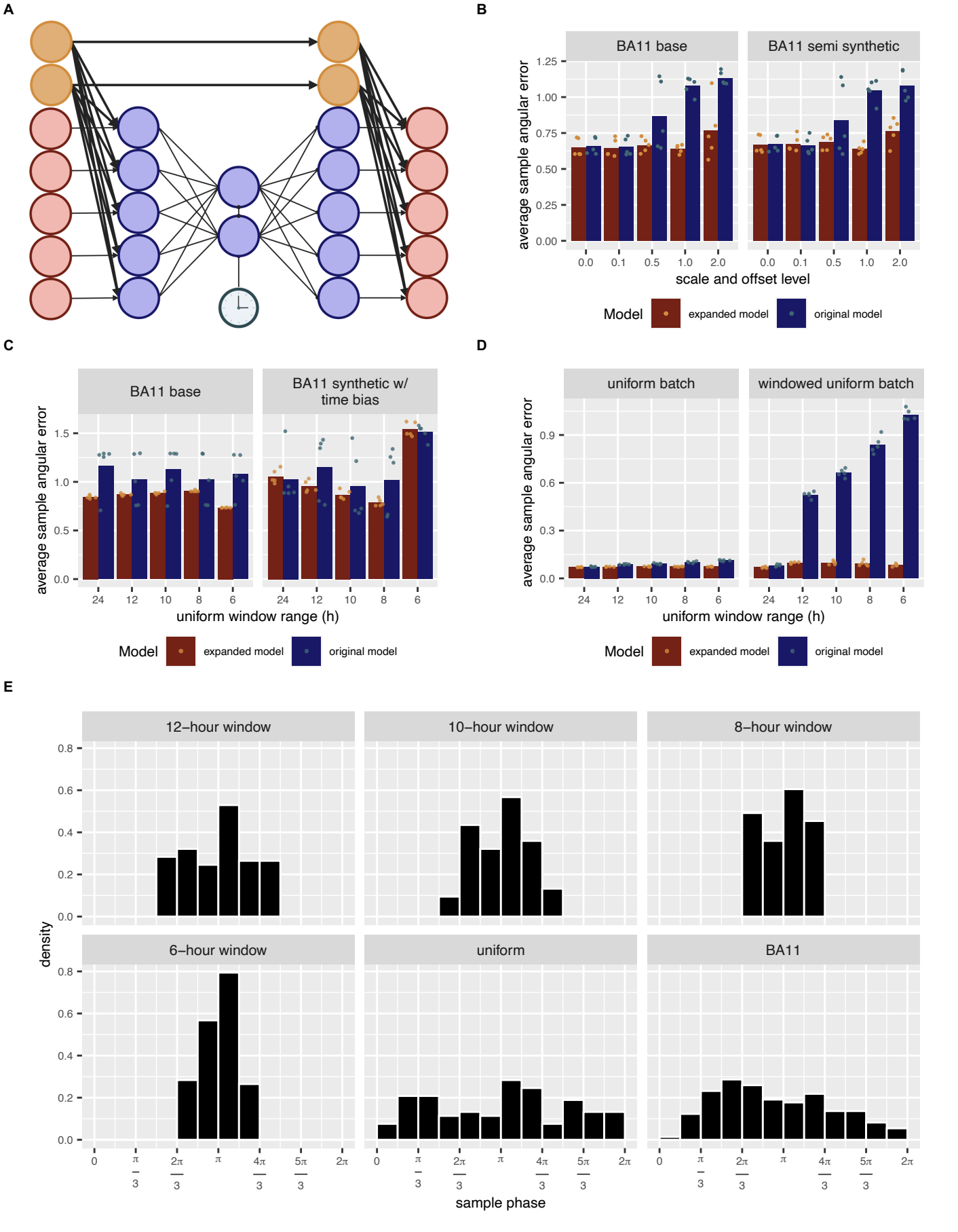
A
B
BA11 base
BA11 semi synthetic
average sample angular error
scale and offset level
Model
expanded model
original model
C
BA11 base
BA11 synthetic w/ time bias
uniform window range (h)
D
uniform batch
windowed uniform batch
E
12–hour window
10–hour window
8–hour window
6–hour window
uniform
BA11
density
sample phase

Fig. S3

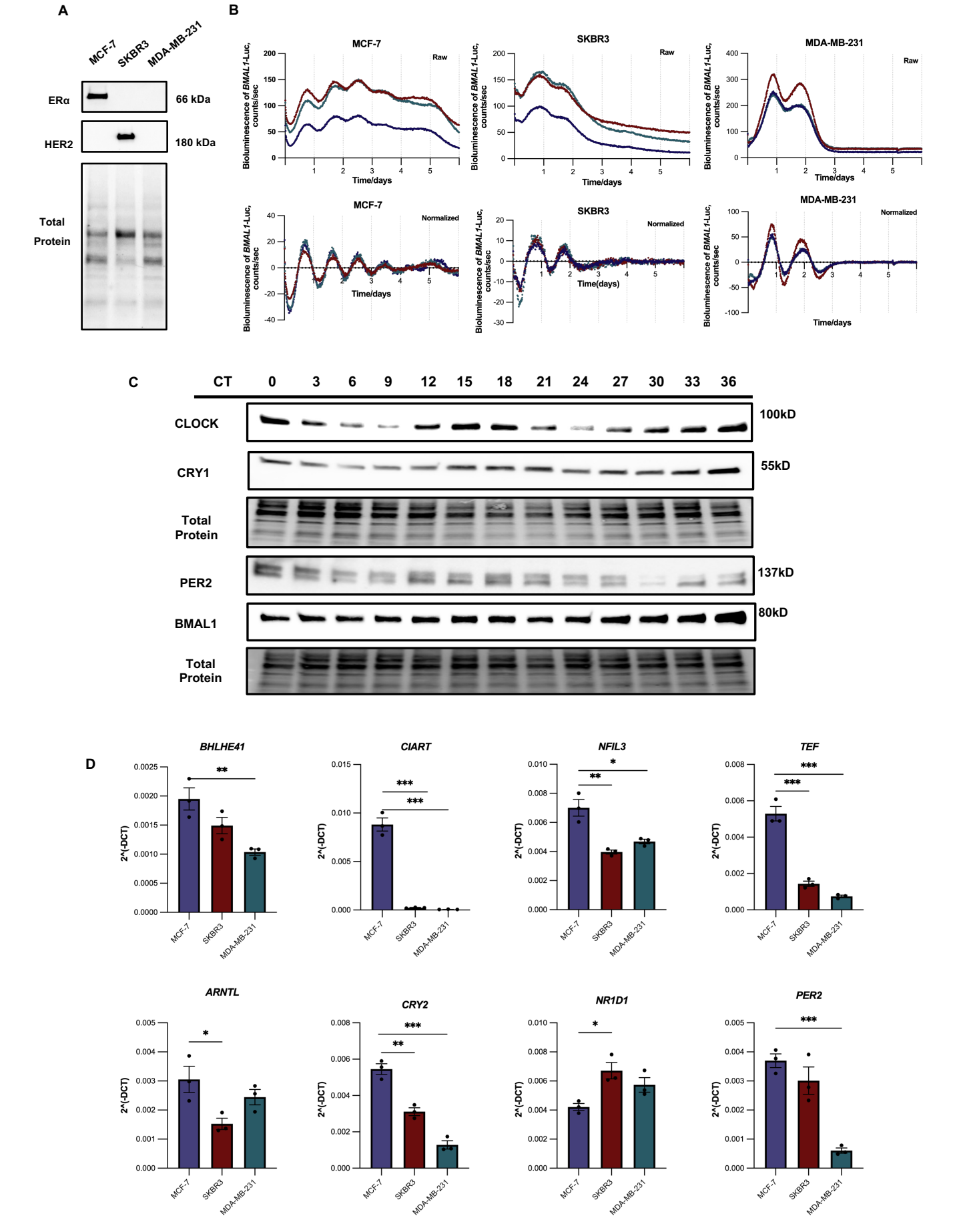
A
MCF-7
SKBR3
MDA-MB-231
ERα
66 kDa
HER2
180 kDa
Total Protein
B
MCF-7
SKBR3
MDA-MB-231
Raw
Normalized
Bioluminescence of BMAL1-Luc, counts/sec
Time/days
Time(days)
C
CT 0 3 6 9 12 15 18 21 24 27 30 33 36
CLOCK
100kD
CRY1
55kD
Total Protein
PER2
137kD
BMAL1
80kD
Total Protein
D
BHLHE41
CIART
NFIL3
TEF
ARNTL
CRY2
NR1D1
PER2
2^(-DCT)
MCF-7
SKBR3
MDA-MB-231

Fig. S4

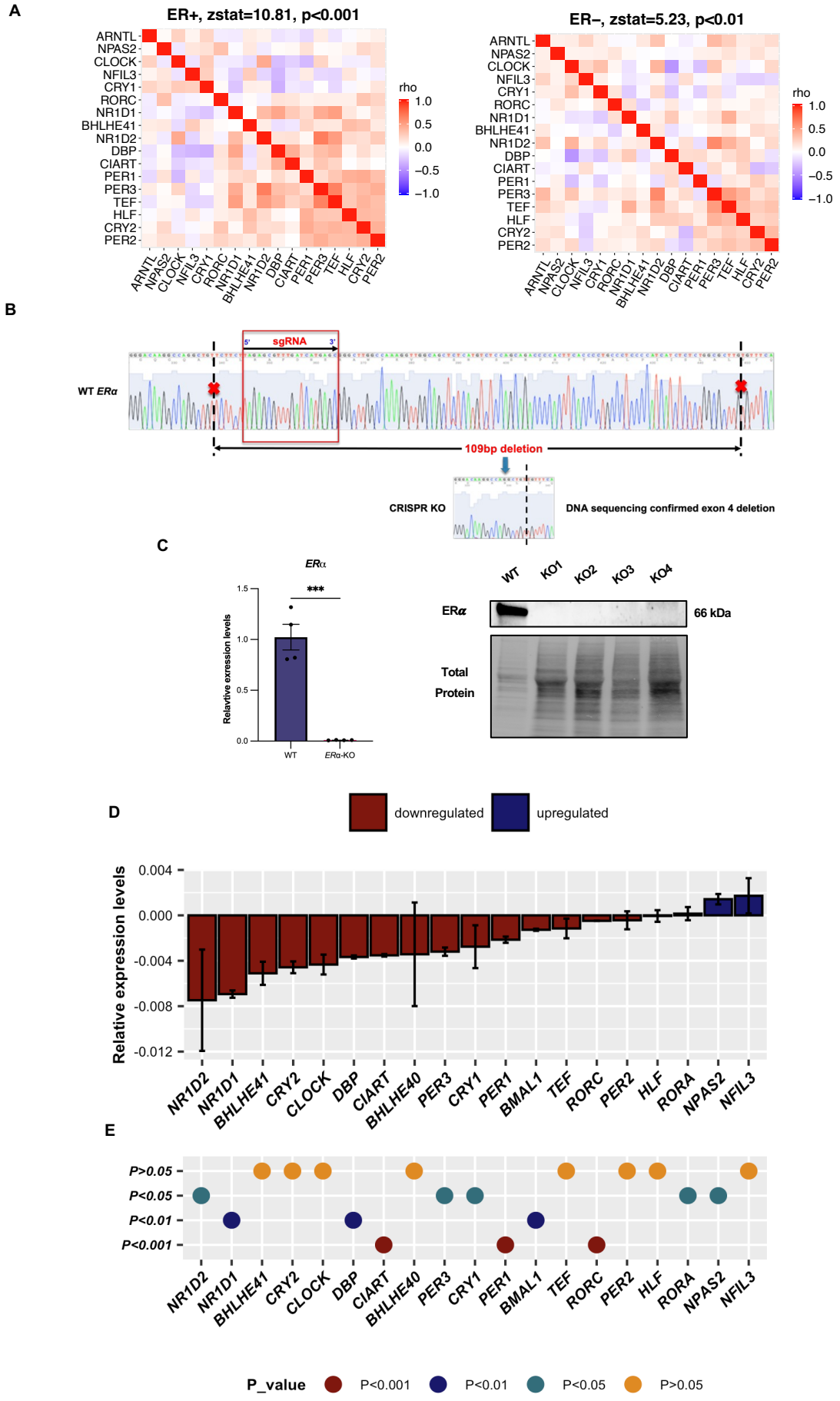
A
ER+, zstat=10.81, p<0.001
ER−, zstat=5.23, p<0.01
ARNTL
NPAS2
CLOCK
NFIL3
CRY1
RORC
NR1D1
BHLHE41
NR1D2
DBP
CIART
PER1
PER3
TEF
HLF
CRY2
PER2
rho
1.0
0.5
0.0
−0.5
−1.0
B
WT ERα
sgRNA
5'
3'
109bp deletion
CRISPR KO
DNA sequencing confirmed exon 4 deletion
C
ERα
***
Relative expression levels
WT
ERα-KO
WT
KO1
KO2
KO3
KO4
ERα
66 kDa
Total
Protein
D
downregulated
upregulated
Relative expression levels
0.004
0.000
-0.004
-0.008
-0.012
NR1D2
NR1D1
BHLHE41
CRY2
CLOCK
DBP
CIART
BHLHE40
PER3
CRY1
PER1
BMAL1
TEF
RORC
PER2
HLF
RORA
NPAS2
NFIL3
E
P>0.05
P<0.05
P<0.01
P<0.001
P_value
P<0.001
P<0.01
P<0.05
P>0.05

Fig. S5

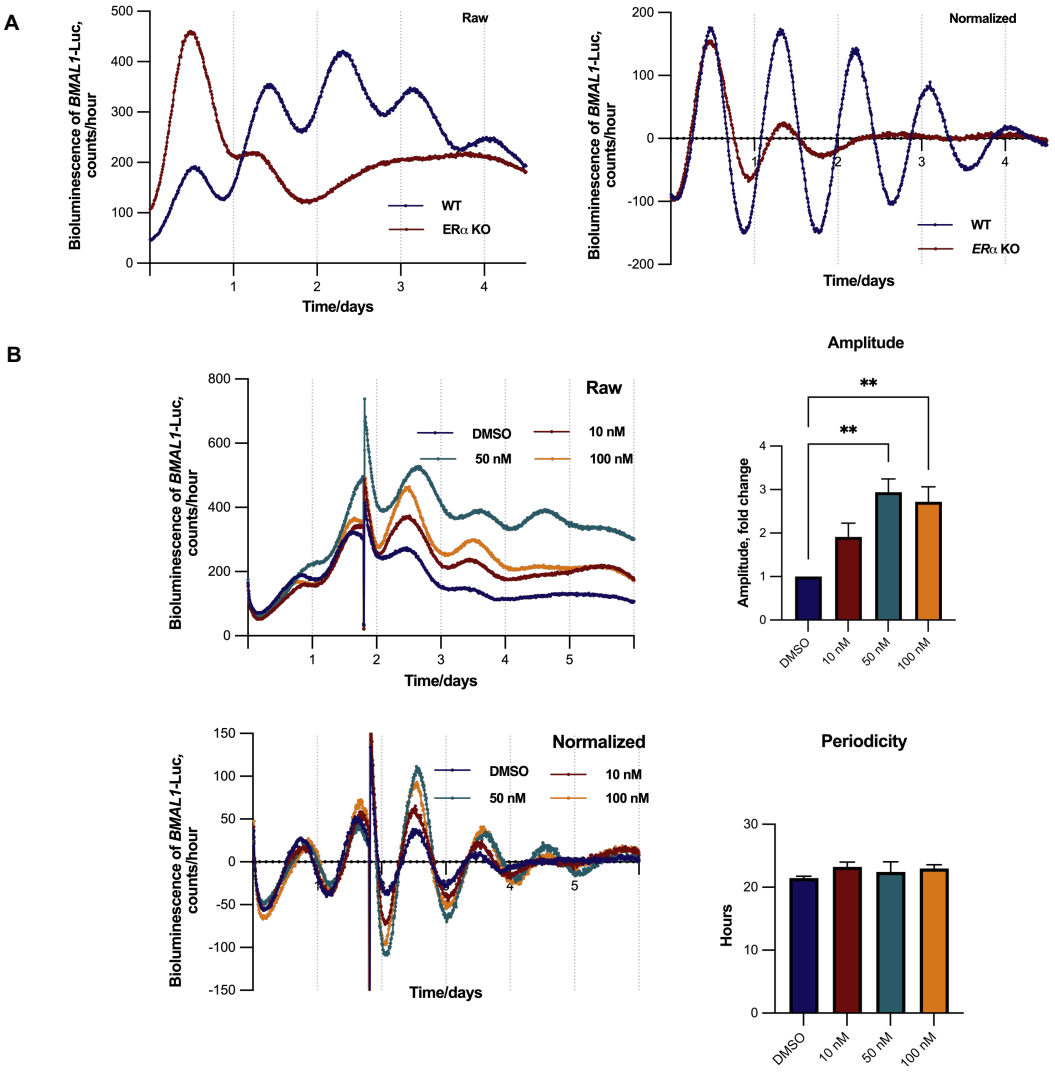
A
Raw
Bioluminescence of BMAL1-Luc, counts/hour
Time/days
WT
ERα KO
Normalized
Bioluminescence of BMAL1-Luc, counts/hour
Time/days
WT
ERα KO
B
Raw
Bioluminescence of BMAL1-Luc, counts/hour
Time/days
DMSO
10 nM
50 nM
100 nM
Amplitude
Amplitude, fold change
**
**
DMSO
10 nM
50 nM
100 nM
Normalized
Bioluminescence of BMAL1-Luc, counts/hour
Time/days
DMSO
10 nM
50 nM
100 nM
Periodicity
Hours
DMSO
10 nM
50 nM
100 nM

Fig. S6

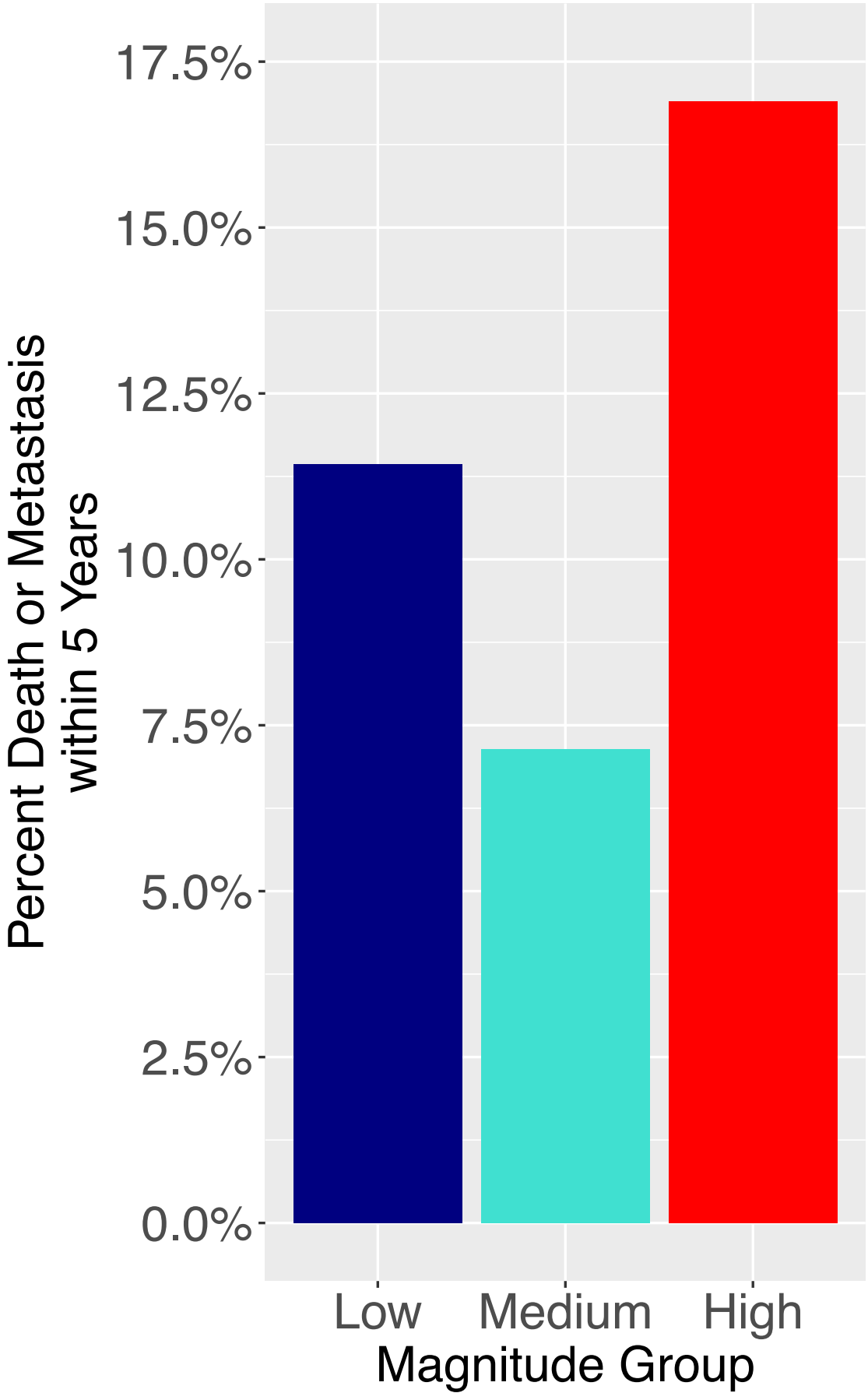
17.5%
15.0%
12.5%
10.0%
7.5%
5.0%
2.5%
0.0%
Percent Death or Metastasis within 5 Years
Low
Medium
High
Magnitude Group

Fig. S7

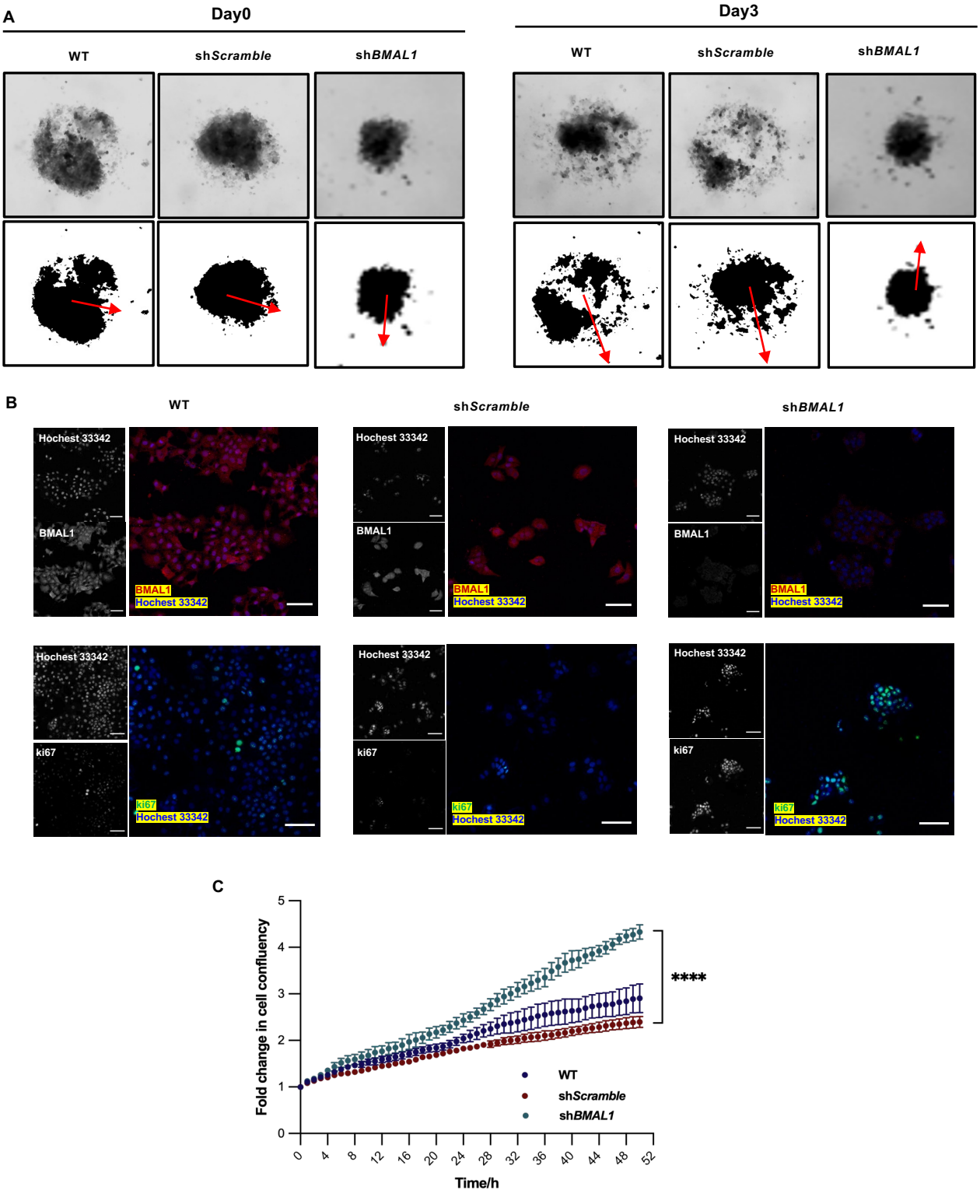
A
Day0
Day3
WT
shScramble
shBMAL1
B
WT
shScramble
shBMAL1
Hochest 33342
BMAL1
ki67
C
Fold change in cell confluency
Time/h
****
WT
shScramble
shBMAL1